Article

The Atmospheric Aerosol over Western Greece-Six Years of Aerosol Observations at the Navarino Environmental Observatory

Hans-Christen Hansson [1,2,*], Peter Tunved [1,2], Radovan Krejci [1,2], Eyal Freud [1], Nikos Kalivitis [3], Tabea Hennig [1], Giorgos Maneas [2,4] and Evangelos Gerasopoulos [2,5]

[1] Department of Environmental Science, Stockholm University, 10691 Stockholm, Sweden; Peter.Tunved@aces.su.se (P.T.); Radovan.Krejci@aces.su.se (R.K.); Eyal.Freud@mail.huji.ac.il (E.F.); Tabea.Hennig@aces.su.se (T.H.)

[2] Navarino Environmental Observatory, Costa Navarino, Navarino Dunes, 24001 Messenia, Greece; giorgos.maneas@natgeo.su.se (G.M.); egera@noa.gr (E.G.)

[3] Environmental Chemical Processes Laboratory, Department of Chemistry, University of Crete, 70013 Heraklion, Greece; nkalivitis@uoc.gr

[4] Department of Physical Geography, Stockholm University, 10691 Stockholm, Sweden

[5] Institute for Environmental Research & Sustainable Development, National Observatory of Athens, 11810 Athens, Greece

* Correspondence: hc@aces.su.se

Abstract: The Eastern Mediterranean is a highly populated area with air quality problems. It is also where climate change is already noticed by higher temperatures and s changing precipitation pattern. The anthropogenic aerosol affects health and changing concentrations and properties of the atmospheric aerosol affect radiation balance and clouds. Continuous long-term observations are essential in assessing the influence of anthropogenic aerosols on climate and health. We present six years of observations from Navarino Environmental Observatory (NEO), a new station located at the south west tip of Peloponnese, Greece. The two sites at NEO, were evaluated to show the influence of the local meteorology and to assess the general background aerosol possible. It was found that the background aerosol was originated from aged European aerosols and was strongly influenced by biomass burning, fossil fuel combustion, and industry. When subsiding into the boundary layer, local sources contributed in the air masses moving south. Mesoscale meteorology determined the diurnal variation of aerosol properties such as mass and number by means of typical sea breeze circulation, giving rise to pronounced morning and evening peaks in pollutant levels. While synoptic scale meteorology, mainly large-scale air mass transport and precipitation, strongly influenced the seasonality of the aerosol properties.

Keywords: atmosphere; aerosol; background; particle size; long term; Mediterranean

1. Introduction

The Eastern Mediterranean area is highly populated area with more than 300 million inhabitants in the countries along the coast from Italy to Libya. This includes major population and industrial centers as the Po Valley, Istanbul, and Cairo having 12–16 million inhabitants each. Considering the large population and industrial activity anthropogenic emissions to the atmosphere is expected to not only affect the major population centers but the whole region as well. Kanakidou et al. [1] show the influence of both gaseous and particulate emissions over the whole Eastern Mediterranean area. The warm climate with high temperature and flux of solar light induce the atmospheric chemistry, giving high concentrations of secondary aerosols. Asmi et al. [2] show the Crete atmospheric observation site Finokalia to have the same number concentrations of Aitken and accumulation mode particles as background stations in Central Europe. Clearly the eastern

Mediterranean background pollution concentrations are considerably higher than over the oceans or larger forest areas and thus could be considered as largely influenced by anthropogenic emissions.

Climate change will probably strongly affect the Mediterranean area not only by increasing temperatures, but more by decreasing precipitation including increasing dry periods and droughts in both Southern Europe, the Middle East and Northern Africa [3]. In Greece the change in precipitation has shown in longer periods of dry weather almost in the whole country especially in the south eastern parts and in the western parts as shorter periods of wet periods when investigating the period 1958–2000 [4]. Similarly, Kostopoulos and Jones (2007) [5] found a significant increase in anti-cyclonic and a decrease in cyclonic weather types.

The decrease in precipitation will affect the atmospheric (particle/aerosol) content, as wet deposition is the major sink for atmospheric particles, i.e., less precipitation will increase atmospheric concentrations of particulate matter. The resulting increase in atmospheric lifetime of particles enhance long range transport of air pollution and dust, allowing for transport from a larger region and thus increasing the atmospheric concentrations. Not only will the air quality be degraded, but it will also impact the direct and indirect effects of aerosol on climate. Increased aerosol concentration will increase the dimming and potentially increase the albedo and lifetime of the clouds. All these effects have the potential to lower the net radiative forcing. However, this does not necessarily have to affect the local or even the regional climate [6].

Besides changes in removal rates, a changing climate can as well affect the aerosol sources, e.g., a drier climate will probably induce increased dust emissions as well affect emissions of organic gases forming secondary particles. Especially during draught large forest fires often occur and release massive amounts of aerosols to the atmosphere. The practice of waste burning in agriculture is another large and common source of air pollution in the Mediterranean region.

It is important to follow how a changing climate will induce changing aerosol concentration through the abovementioned changes in sources and sinks, as well as how anthropogenic emission contribute to the burden of particles in the Mediterranean region. This information is pertinent to facilitate projections of how the Mediterranean climate and air quality will evolve, and is further required for the development of co-beneficial cost-effective abatement plans as the present climate and air quality at times cause considerable problems and strain to human health.

Comprehensive long-term background observations of the air pollutants including the aerosols are quite sparse in the Eastern Mediterranean, especially when compared with Northern Europe. ACTRIS, the European Research Infrastructure for the observation of Aerosol, Clouds, and Trace gases in Europe is composed of observing stations, exploratory platforms, instrument calibration centers, and a data center. The only long-term site in the Eastern Mediterranean within ACTRIS is Finokalia at Crete. Recently a site at Cyprus has been added to the network (www.actris.eu, accessed on 6 March 2021). There are many sites recording PM10 and/or PM2.5 especially in urban environments, however most of these sites do not observe chemical composition and almost none measure particle number and their size distribution which are necessary to not only determine major sources but also reveal major processes affecting transport and sinks and thus concentrations. However numerous short-term campaigns have been performed investigating atmospheric conditions, sources, transport and sinks including, e.g., Helmis et al. [7], who investigated the contribution from long range transport to sulfur and nitrogen compounds into Greece. Other phenomena have been attracting the attention of the scientific community. This includes a variety of sources [8], the intense photochemical aging [9], and the interactions with the marine environment [10]. Several studies have focused on chemical composition of the atmospheric aerosol in the region, in urban/suburban environments [11,12], rural [13], and background conditions [14,15]. Still, studies of physical properties and especially

number size distributions remain scarce, and most of the existing studies relate to the island of Crete and the Finokalia station.

From the early studies it was already shown that even if Finokalia is representative for the marine background conditions, however, due to the rapid transformations of aerosol in the Mediterranean atmosphere, microphysical processes may better be observed at distances closer to the pollutant sources, at around 100 km distance [16]. Lazaridis et al. (2006) [17] showed, based on two field campaigns studying aerosol number size distributions, that Eastern Mediterranean basin is moderately to highly polluted during the summer and relatively unpolluted during the winter. Kalivitis et al. (2008) [18] also demonstrated a strong influence on size distributions in air masses originating from continental Europe compared to marine air masses. Kalivitis et al. (2019) [18] additionally suggested that new particle formation is not as frequent or intense as for continental sites in summer. Kopanakis et al. (2013) [19] showed for the Akrotiri site, western Crete, that aerosol size distributions were clearly season dependent, with peaks of number in the larger diameter range during summer and spring. Pikridas et al., (2012) [20] reported higher frequency of new particle formation events during winter and less frequent during summer. Petäjä et al., (2007) [21], focusing on the urban environment in Athens, demonstrated that new particle formation was common in the urban environment of Eastern Mediterranean as well, and based on hygroscopicity measurements during urban pollution events, growth of nucleated particles due to condensation of water-soluble material dominated. New particle events have also been reported as a frequent observation at the urban environment of Thessaloniki [22]. Kalivitis et al. (2015) [23] suggested that new particles do grow in eastern Mediterraean to cloud condensation nuclei (CCN) sizes based on aerosol size distributions and CCN measurements while Kalkavouras et al. (2017) [24] reported that new particle formation may result in higher CCN numbers, but the effect on cloud droplet number is limited by the prevailing meteorology.

Long-term measurements create the necessary basis required to study key atmospheric chemical and physical properties, and how they vary on a diurnal, seasonal, annual and ultimately on decadal time scale. This allows an evaluation of the influence of meteorology, sources, transport and sink variability on the atmospheric composition (e.g., Tunved et al.) [25] but also provides suitable data for an in-depth comparison with and/or evaluation of atmospheric chemistry transport or climate models.

The Navarino Environmental Observatory (NEO) is placed on the southwest coast of Peloponnese about 7 km north Pylos. NEO was established in 2010 as a common effort between the Greek private company TEMES S. A., a developer of environmentally sustainable resorts, the Biomedical Research Foundation of the Academy of Athens and Stockholm University, to perform research and education on the climate and environment in the Mediterranean region. The atmospheric program was established in 2011 to contribute with observations needed to better estimate the influence of air pollution in the eastern Mediterranean and its influence on climate.

In this study we evaluate long-term observations of the atmospheric aerosol number size distribution in terms of sources, sinks and transformation processes in the Eastern Mediterranean with special focus on Peloponnese and the Adriatic and Ionian Sea, based on datasets from two NEO sites located in southern Peloponnese. The influence of the placement, local meteorology and sources are also evaluated and discussed at length. At the first location (the Navarino site, 36°59′46″ N, 21°39′00″ E, elevation 35 m, distance from the coast 880 m), the 2.5-year dataset (April 2011 to October 2013) consists of data on aerosol number size distribution in which local and long distant transported aerosol is identified and characterized. However, the data was questioned due to possible local influence, and in the fall 2013 the measurements were moved about 21 km south, to a meteorology station, operated by the Hellenic National Meteorological Service, in the vicinity of the village Methoni on the south tip of the most western peninsula of Peloponnese sticking out into the Ionic Sea. The Methoni site, (36°49′30″ N, 21°42′17″ E) is secluded on a cliff 20 m above sea level and about 400 m from the shore line and with the small village Methoni situated

to the South East and thus mostly down wind. Having another three years of observations from the Methoni site (2013–2016), besides comparing the two sites, we can investigate and discuss the role of different processes controlling the aerosol size distribution on longer and shorter temporal scales for the both sites. By performing trajectory analysis and transport statistics, we identify long-distance transported aerosol sources and effects of sinks and transformation. We also provide an explanation of the variability observed as well as the influence of local sources and general characteristics of the two sites. The data analysis is divided in two major segments: one focusing on seasonality of aerosol and role of source areas and local meteorology. Second part focus on clustered aerosol size distributions and relation to meteorological history, including precipitation and transport patterns.

The results show the geographical placement of an atmospheric observatory is important and consideration has to be taken to local and regional topography before establishing a site as it is influencing both regional and local meteorology and thus air pollution transport. Besides reporting typical atmospheric particle concentrations for the area, the results once more show how strongly long distant transported air pollution not only from nearby sources but from all Europe affects the air quality and climate of all European regions.

2. Description of Sites

The first set-up of air observations at the Navarino Environmental Observatory (NEO, see Figure 1) was installed April 2011 in a tower building at the Navarino Dunes, Costa Navarino Resort, about 300 m from the sea side, with an inlet about 7 m above the roofs of the hotel buildings. This site is below referred to as "Navarino". In the wind sector WNW to NNW there was no emissions from ventilations or heating facilities in the resort. However, during the measurements there have been concerns that due to turbulence over the buildings influence from kitchen vents might influence the sampling. To minimize the risk for local contamination the air observations were moved end of September 2013 to the old meteorology station at Methoni about 21 km SWS Navarino to minimize the risk for influence of local pollution.
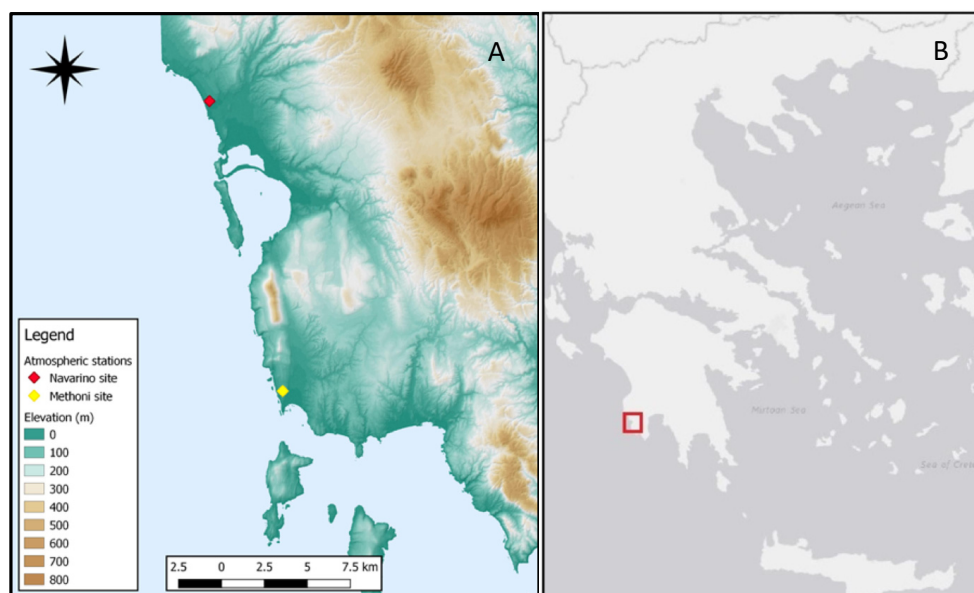

Figure 1. Map **A** showing Messina, the southwest region of Peloponnese (mark with a red square in Map **B**), in the south west of Greece. NEO is situated at the coast about 11 km north the nearest city Pylos. The Methoni site is about 11 km south Pylos.

The instrumentation was installed in October 2013 at the meteorology station situated NW of the village Methoni. The station is placed on a cliff some 30 m above and some

400 m from the shore line. The sector NNW to SSW is unpopulated, without any roads and fully open towards the sea.

3. Methods

3.1. Instrumentation

The measurements of the aerosol number size distribution were conducted with a custom build DMPS system consisting of a medium size Vienna type DMA [26]. The DMAs were operated with flow ratios of 1:10. The CPC was a TSI CPC3772. The DMPS systems could cover the size range from 20 to 956 nm in particle diameter. In addition to the option of measuring the aerosol particle size distributions the system could measure the total particle concentration. The measurements of the total particle concentration and the particle size distribution were conducted sequentially. The measurement system was fitted with Perma Pure nafion dryers in the aerosol line and the sheath air lines of the DMA that were run with dried air provided by a Kaeser DENTAL T1 compressor.

Throughout the system the following parameters were monitored: the aerosol air flow and the excess air flows using SENSOR TECHNICS BTEL5000 differential pressure sensor, the relative humidity in the aerosol air flow and the excess air flow using VAISALA HMT330 capacity sensors, and the system pressure using SENSORTECHNICS 1444SB001A-PCB barometric pressure sensors.

The inlet, PM10 design, is placed 2 m above the top of the tower, which is about 5 m above the general roof top height at Navarino placing the inlet about 30 m above sea level. At NEO the instrumentation is a placed in a container closest to the beach cliff at the meteorology site. The inlet is placed about 2 m above the container roof.

Meteorological parameters were continuously monitored during the operation of both sites with the use of automated meteorological stations. In particular, at the Navarino site the station was set up in August 2010 (wind speed and direction reference 3 m from the ground) measuring the following parameters: precipitation, temperature, relative humidity, wind speed and direction). The transport of the station at Methoni was followed with the setup of new meteorological instrumentation in January 2016, which included the monitoring of the following parameters: precipitation, temperature, relative humidity, wind speed and direction, radiation (wind speed and direction reference 6 m from the ground).

3.2. Data Processing and Analysis Tools

3.2.1. Data Treatment

Aerosol size distribution data between 20 and 920 nm have been manually screened for inconsistencies, maintenance and instrumental errors according to the ACTRIS routines (ACTRIS. Available online: http://www.actris.eu/ (accessed on 12 March 2021). The background air, daily plus night, was chosen from inspecting monthly total number plots excluding the local pollution emerging as increased concentration in the morning and evening. After screening of data, roughly 17,000 hourly average values were calculated for the Navarino site, while the new site location resulted in around 7000 hourly average data points. The reasons for this discrepancy in data coverage is the increase in instrumental malfunction due to more harsh sampling conditions experienced at the Methoni site.

3.2.2. Lognormal Fitting Procedure

The data were fitted with three lognormal modes for the hourly averaged data. Fitting was performed for size distribution data between 20 and 580 nm in order to assure that the analysis was performed on a data set with identical size range for the studied period. The fitting routine adapted utilize the fmincon.m function in Matlab to perform a constrained fit of each size distributions into three lognormally distributed modes between 20–630 nm. We do not select any distinct modal range a priori, but instead allow the algorithm to find the best mathematical solution that captures the overall shape and magnitude of each individual size distribution. After fitting each size distribution, the three modes were arranged according to size, and in the following we refer to the three modes as

nuclei, Aitken and accumulation mode (i.e., mode 1–3). This terminology can be somewhat misleading, as the fitting do not force either of the modes into a prescribed size range. This means that, e.g., the smallest mode of any fit always will be referred to as nuclei, regardless of its actual size. Thus, some deviations from the conventional size range of the modes will occasionally be apparent. Bearing in mind that the fitting is based on best semi-constrained fit (20–630 nm), we do however still think that the chosen approach serves the purpose of the study. A total of about 24,000 individual size distributions have been fitted in this way.

3.2.3. Trajectory Calculations

Throughout the studied period, hourly 240 h back trajectories were calculated using the HYSPLIT4 model [27]. The trajectory calculations are based on one-degree meteorological data from the GDAS (Global Data Assimilation System) data set (cf. Gridded Meteorological Data Archives. Available online: http://ready.arl.noaa.gov/archives.php (accessed on 12 March 2021)). The trajectories are used to estimate spatial distributions of the potential source areas that define the aerosol properties at NEO. The same trajectories are also used to study the air mass history in terms of precipitation intensity, which is supplied as optional hourly output along the calculated trajectories. Each hourly average of aerosol number size distribution was in this way coupled with corresponding 240 h airmass back-trajectory, providing both spatial "footprint area" of the number size distributions as well as modelled meteorological output from the trajectory simulations, including altitude, temperature, relative humidity and precipitation intensity.

3.2.4. Cluster Analysis

The use of clustering in the analysis of aerosol size distribution have found application in several studies focusing on the aerosol lifecycle and as well as in different process studies a wide range of environments [28–31]. Clustering of size distribution serves as an efficient way of identifying "signature" aerosol number size distributions. By linking the meteorological history and regional transport pattern of airmass trajectories to the different clusters, substantial amount of information can be extracted that allows for better understanding of the processes and sources at play in shaping the observations at the receptor.

In the current study we have used the kmeans.m clustering function available in the Matlab Statistics and Machine learning toolbox, and in doing so we applied the squared Euclidean distance function. When clustering size distributions, one may either choose to cluster the size distribution as is, i.e., with actual observed number concentration, or after a normalization of the number size distribution data, the shape of the size distribution. In this study we have used the latter approach, and the size distributions were normalized to their respective peak value, yielding aerosol number size distribution values ranging from zero to one. In this way the main focus will be on shape, and biases due to extremely high concentrations will be reduced.

In the current study, only a subset of data (only observations between 9:00 and 15:00 UTC) was treated using cluster analysis. The data clustered included only size distribution data between 20 and 580 nm, which correspond to the largest common size range during the period of study. This subset was selected based on the preliminary analysis of aerosol number size distribution observations at the different locations to distinguish the true regional background as opposed to locally influenced airmasses frequently observed at the Navarino measurement site. A more comprehensive discussion on how this selection was made is given below in the analysis of the local meteorology. The number of clusters was chosen to six, and this number seems to capture the different stages in the aerosol lifecycle well.

4. Results

The Navarino Environmental Observation, NEO, site is a new observatory, which has to be evaluated concerning the influence of local sources of air pollution to reveal how

useful the measurements are for characterization of the background aerosol in the Adriatic Sea and surrounding areas. The local influence is evaluated through examining the diurnal and seasonal variations, which is presented below.

4.1. The General and Local Meteorological Situation

The Mediterranean basin lies between the sub-tropical and the mid-latitude zone. The strongly varying orographic features together with land-sea interactions further complicate the meteorology resulting in large variability of weather types shaping the regional climate accordingly. Kostopoulos and Jones [5] found large scale synoptic systems in the northern latitudes to influence the winter and spring climatic conditions in the eastern Mediterranean giving mainly a northerly dominated wind flow. Further the smaller scale low-pressure systems over the Mediterranean Sea associated with high precipitation plays also an important role in the winter and spring. The summer meteorology is largely dependent on the Azorean High and the Asian summer Low giving a dominantly dry and warm climate with dominating northerly wind flow, ranging from WNW to NE, while the fall is mainly a transition period between the cold and warm period with alternating features typical for the warm and cold periods [5]. By this, the annual weather cycle in Greece can be divided into two major periods, the warm and dry summer, May–September and the cold and wet winter period, November–March with April and October as transition months.

4.2. Air Mass Transport

In order to study transport patterns during the measurements, the result from the trajectory calculations was used to create a transport probability function. This was realized by creating a polar coordinate system consisting of 180×180 grids centered around the receptor stations. The transport probability function describes the likelihood of a randomly selected trajectory crossing a certain cell in the grid system as:

$$p\left[A_{ij}\right] \; = \; \frac{n_{ij}}{N} \tag{1}$$

where n_{ij} is the number of trajectories crossing cell (ij) and N is the total number of trajectories.

The trajectory data was subdivided into three different periods, resulting in one transport probability function for the warm period (May–September), one for the cold period (November–March) and one for the transition period (October and April). The result is displayed in the top panels of Figure 2. In addition to the transport probability function, the average altitude of each trajectory was mapped in a similar manner, providing the typical altitude the air parcel travels at over each grid. This aids the analysis of how the trajectories are transported in the vertical, and to what extent they are exposed to ground level emissions versus high level transport. The results are shown in the bottom panels in Figure 2.

As can be seen, the warm period (May–September) is characterized by transport dominated by air masses coming from the north along the Adriatic Sea, i.e., from the central Europe. However, it should be noted that it originates from air at about 1500 to 2000 m altitude over central Europe and through subsidence brought to sea level at NEO, and the influence from surface sources is likely low.

The general airmass transport pattern during the cold period is different. Transport is more frequent in the NE sector, as shown in Figure 2. This transport direction is characterized by relatively more pronounced low-level transport, suggesting more contact to the surface and sources. The transport in the NW sector over the Adriatic Sea is less frequent during the cold period, and average altitude in this sector is also lower compared to the W. The transport over the Mediterranean Sea is according Figure 2 dominated by low level transport during the cold period but even more during the warm period. The transition period (October and April) share features with both the cold and warm period, i.e., one pronounced NE leg and one NW leg.
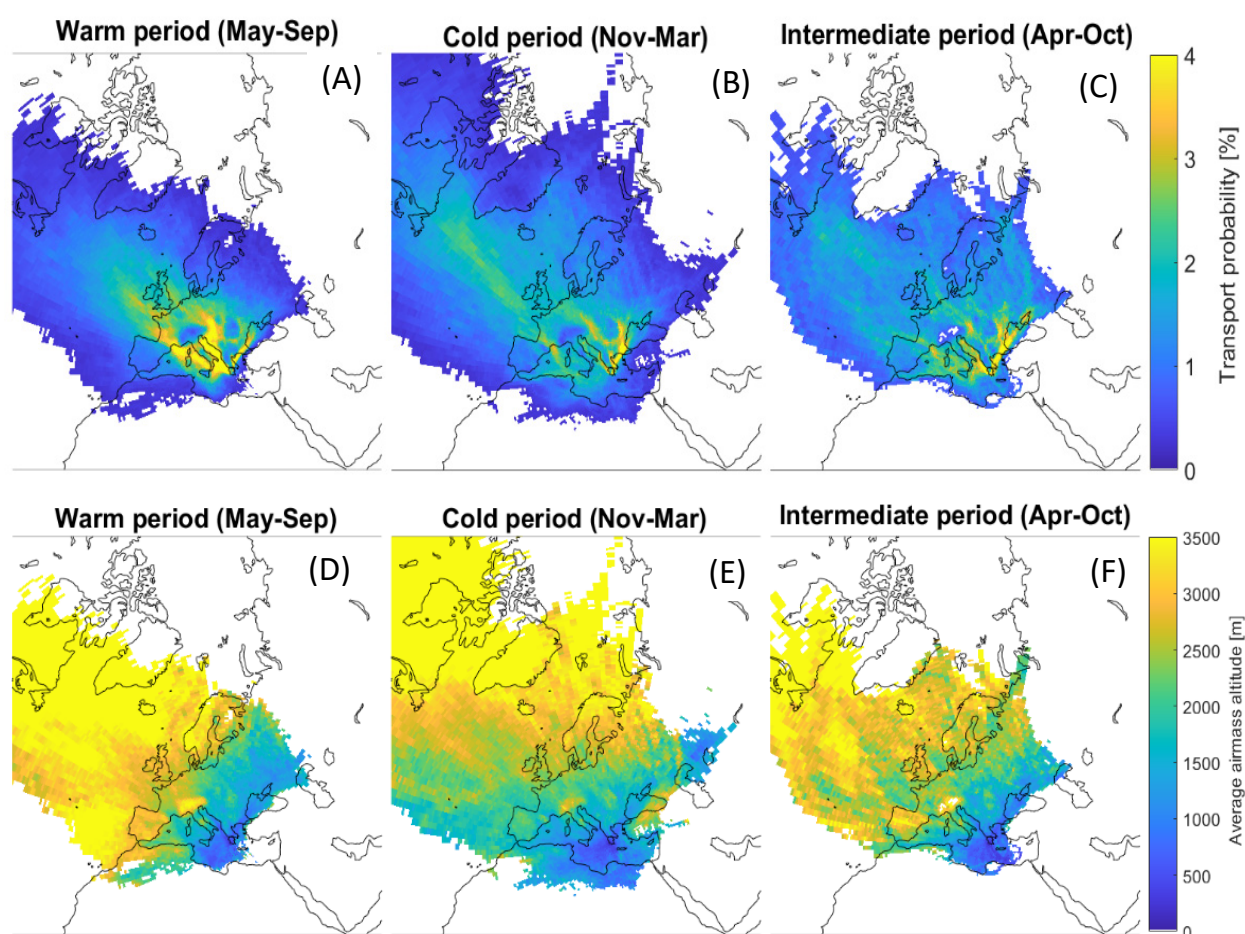
Figure 2. Top panel; Transport source area characteristics, last 240 h, for the warm period, May–September (**A**), cold period November–March (**B**) and transition months April and October (**C**). Bottom panel; Transport average altitude characteristics, last 240 h, for the warm period (**D**), cold period (**E**) and transition months (**F**).

These results agree very well with the general meteorology described in literature reviewed above showing that both during the warm and cold period the prevalent synoptic situations cause generally an air mass transport from Central and Eastern Europe, respectively over the Eastern Mediterranean area.

4.3. Local Meteorology

While the trajectory analysis reflects the synoptic transport conditions, an analysis of local meteorology is needed in order to fully understand the local to mesoscale meteorological features such as sea-breeze circulation shaping the meteorological characteristics at the Navarino and Methoni sites.

The wind roses in Figure 3 show the hourly average wind directions per month for Navarino (3a) and Methoni (3b). As can be seen, there are two local dominating wind directions. Winds from W to NW are the most frequent at both sites with wind speeds usually in the 2–10 m/s region with Methoni generally having stronger winds. At Navarino the other dominant wind direction is NE to E, with wind speeds below 1 m/s (see Figure 3a). The westerly winds are only interrupted by occasional SE winds. At Methoni the other dominating wind direction is slightly more northerly with wind speeds in the range of 2–4 m/s (see Figure 3b) occasional winds from ESE. Thus, two main wind sectors can be identified; one WNW with comparably high windspeeds and one ENE sector with typically lower windspeeds. On average, Methoni experiences higher windspeeds compared to Navarino.
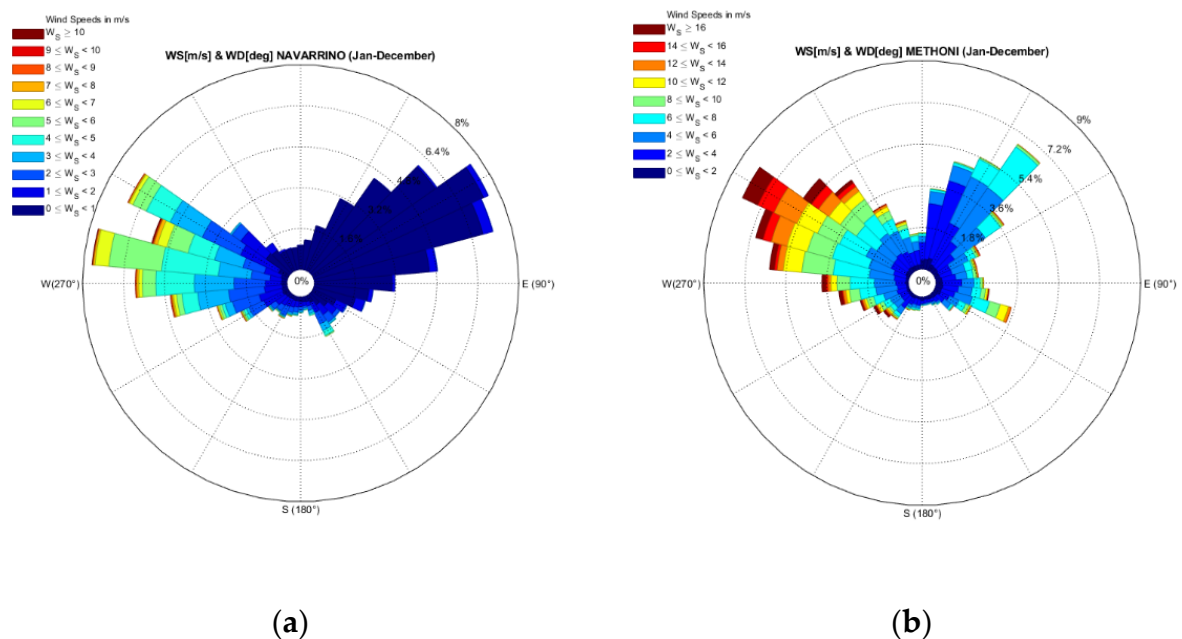
(a)   **(b)**

Figure 3. (**a**,**b**) a/Local wind roses for Navarino (left panel) and b/Methoni (right panel). Navarino 2011–2013 and Methoni 2014–2016.

Subdividing the data into the two main time periods (warm and cold periods), and into day and night a seasonal diurnal variation in typical night and day wind patterns becomes evident at both sites (Figure 4). As can be seen, daytime in both periods are characterized by the dominant WNW wind direction except for Methoni that during the cold period has at times a ESE wind. Methoni as well has generally higher windspeeds. At night time both sites are dominated by slow NE flow but Methoni during the warm period is equally exposed to stronger winds from the NW. It is striking how stable both the general and the local winds are through the different seasons.

In coastal regions with high incident solar radiation, the sea and land breeze typically dominate the local to mesoscale circulation and the sea-land breeze becomes a superimposed feature on the regional wind flow giving a daily steady breeze from the sea changing into a very slow wind from the inland of Messina during nighttime (see Figures 5 and 6). However, this pattern is different at Methoni which is probably due to being placed on the point of the peninsula sticking out into the Ionic sea. During the cold period Methoni often during daytime experience a slow breeze from the ESE coming along the southern coast of Peloponnese. During the warm period, the land breeze does not always develop as at Navarino. The breeze from NW at Methoni continue through the night equally often as turning to the NE as at Navarino.

The sea-land breeze at Navarino is supported by the topography with a mountain range following the coastline of Peloponnese about 10 km inland with a varying height of 300 to 1200 m asl. The sea-land breeze will bring the emissions from the coastal areas into the upper part of the boundary layer during the day circulating out to sea mixing with the

General flow mainly coming from the north along the Adriatic Sea giving a mixture of long distance transported air pollutants and emissions of air pollutants along the coast of Croatia and Greece. During the night the mixed long range and more recent emissions slowly subsiding over the coastal areas going with the land breeze to sea. However, during the shifts there is no wind causing the very local emission to accumulate and dominate the observed air pollutant concentrations. Even when the major flow is from the ENE the mountains in the Peloponnese probably induce considerable turbulence forcing it to skew and subside into a NW flow at lower altitudes towards Navarino and Methoni (see Figure 3). The boundary layer height has been measured to about 1200 m decreasing to about 800 m during night in summertime.
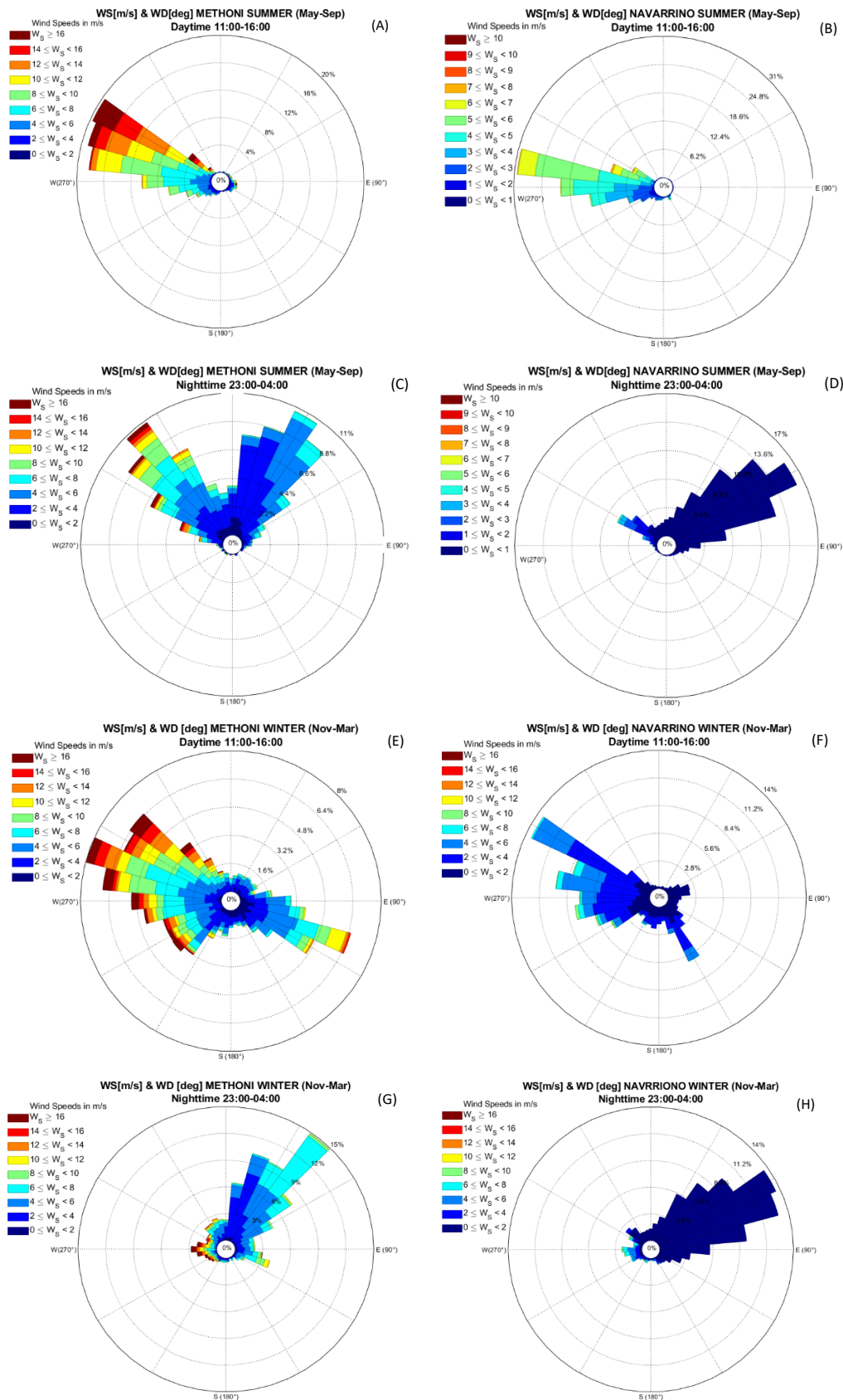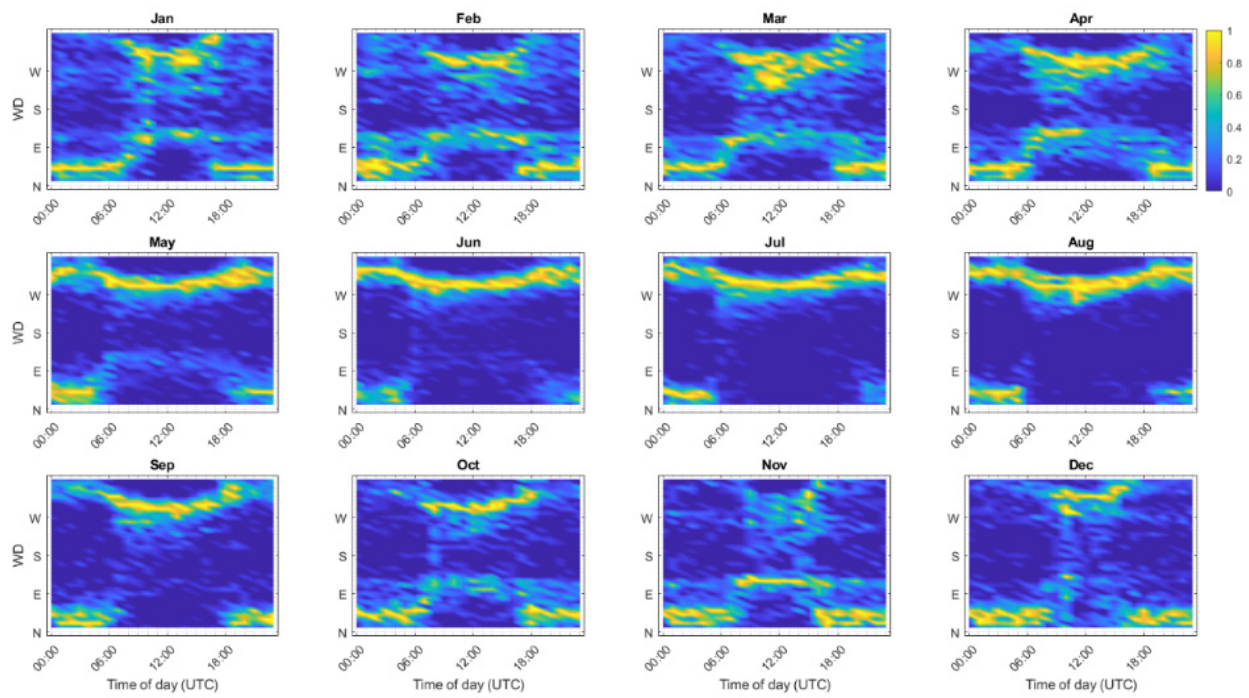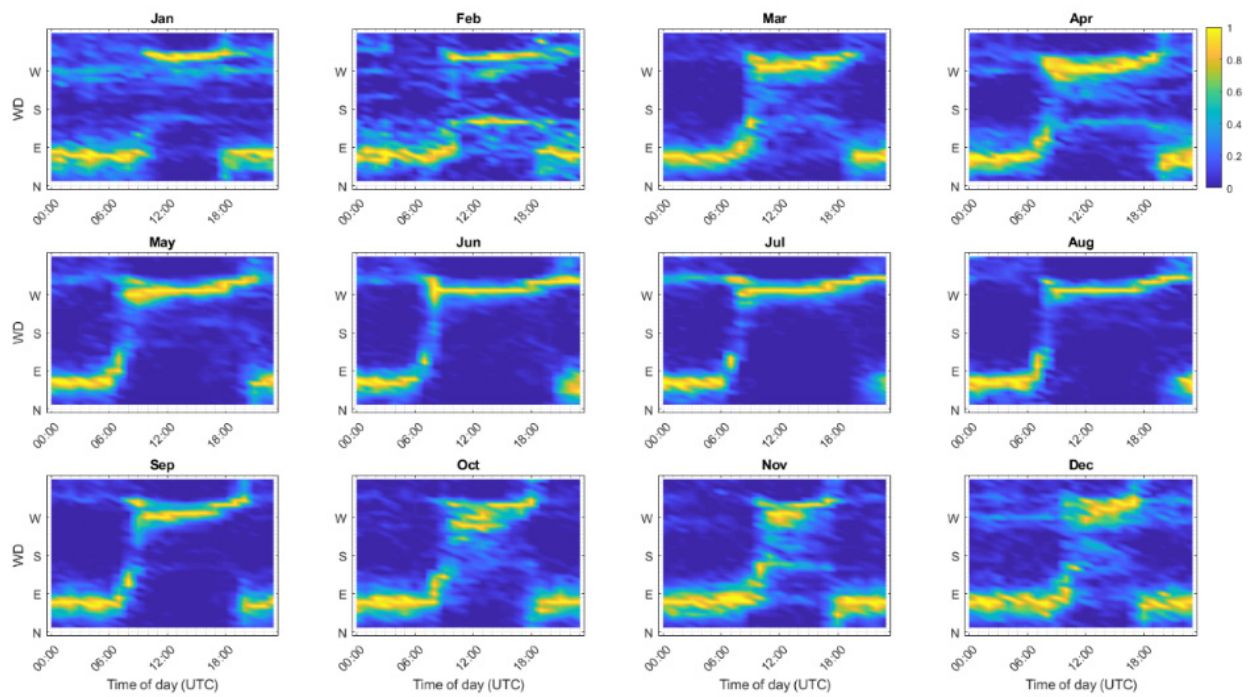
Figure 4. Local wind roses for Methoni (**A**,**C**,**E**,**G**) and Navarino (**B**,**D**,**F**,**H**). The warm season daytime is on the top row while night time is 2nd row. The wind roses for the cold season daytime is 3rd while nighttime is on the 4th row.
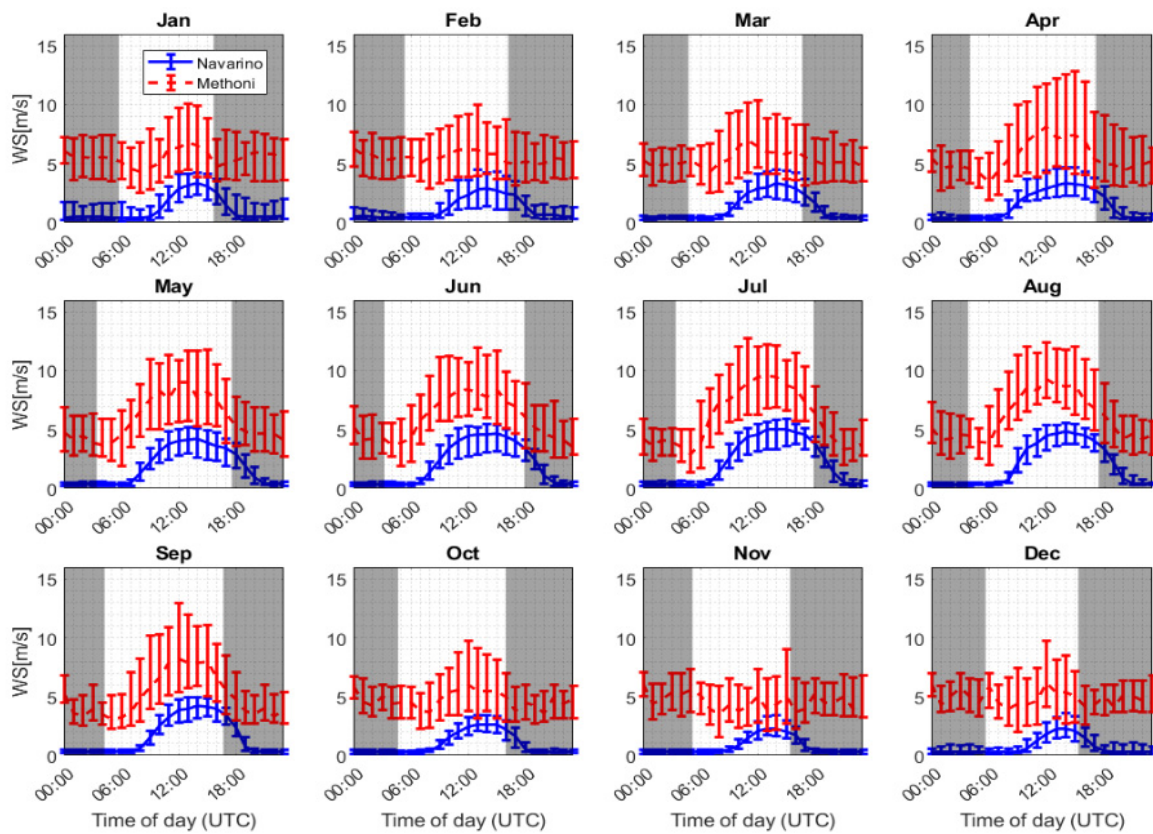
(**a**)

(**b**)

Figure 5. *Cont.*

(**c**)

Figure 5. (**a**) The monthly frequency of local wind directions per hour at Methoni, November 2013 to December 2016. (**b**) The monthly frequency of local wind directions per hour at Navarino, April 2011 to October 2013. (**c**) Monthly median hourly local wind speed for Navarino, April 2011 to October 2013 and Methoni, November 2013 to December 2016, with the 15 to 85 percentile range indicated by the vertical bars. The grey parts show the period when sun is below horizon.
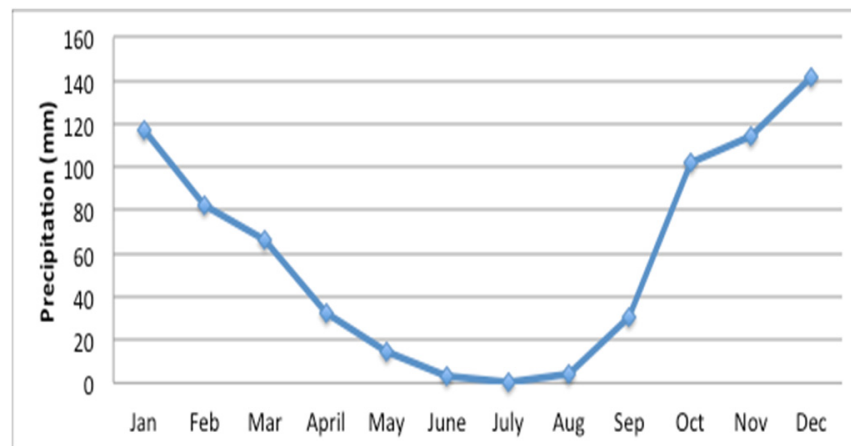

Figure 6. Monthly precipitation at Methoni, Peloponnese (data source: Hellenic National Meteorological Service-HNMS).

The sea-land breeze circulation is a consistent feature during the whole year, only somewhat weakened during October to December. The shift as observed in wind direction at Navarino (see Figure 5b) between land-sea to sea-land breeze occurs about 2 h after sunrise. This shift is delayed somewhat during October to December. The shift back in the evening occurs about within 2 h after sunset during the warm period, i.e., May to

September while during the rest of the year it occurs within an hour after sunset. The wind speed during the day reach about 4–5 m/s during the warm period while it is somewhat lower, about 2–3 m/s during the rest of the year (Figure 5c). At Methoni, the sea breeze during the warm period equally often is interrupted during night by a NEN wind except during June when the sea breeze is still steady through the night (Figure 5a). The wind speed slows down during night but not below 2 m/s (Figure 5c). During the cold period the wind direction is WNW or ESE mostly during the day but change during night time to NE, but the wind speed stays consistently at about 2–3 m/s (Figure 5a,c).

The precipitation as measured at Methoni has a strong seasonal variation with low precipitation, totally about 50 mm during the warm period while totally about 655 mm during the rest of the year (Figure 6). This infers a much stronger sink for aerosols and water-soluble gases during the cold period.

4.4. Aerosol Mode Number Concentrations

The local meteorology at Navarino with the sea-land breeze and thus a change of wind direction twice a day giving periods of no wind inevitable cause a strong influence from local emissions. The increase in median concentration and inter quartile range of total number of particles show clearly high concentrations at Navarino occur in the morning, the late afternoon and early evening (see Figure 7). This is concurrent with low wind speed and shift in wind directions decreasing the dilution of the local emissions (see Figure 5a–c). The stagnant conditions allow the buildup of local pollutants, and the close proximity to anthropogenic sources at Navarino compared to Methoni contributes to this pronounced diurnal variability. However, at Methoni, there is a very small diurnal variation indicating that the local influence is considerably less. This leads to the conclusion that the more dominating NW wind direction and higher wind speeds decrease the influence of local pollution sources and can be considered representative for a larger region.
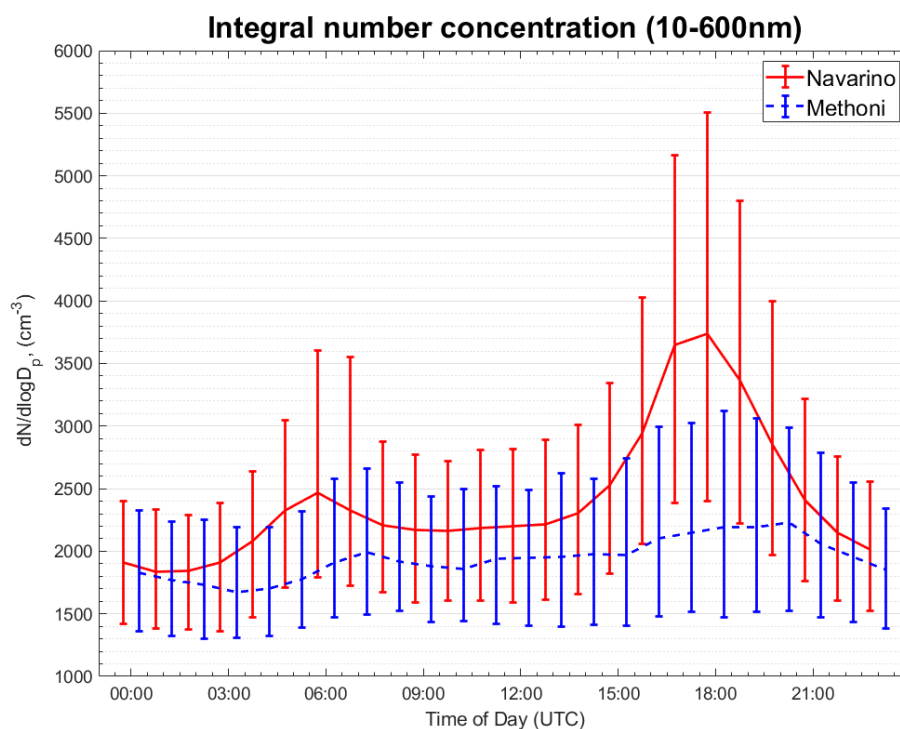

Figure 7. The diurnal variation of the total particle number concentrations at Navarino (observations for the period April 2011–September 2013) and at Methoni (observations for the period November 2013–December 2016). The lines indicate the median values while the error bars indicate the inter-quartile range.

When separating the total number into different modes (see Appendix A) and into the different seasons previously described both the Aitken and accumulation modes do not differ in number at the two sites between 9 and 15 UTC during the cold period (Figure 8). Together with the findings with respect to diurnal cycle of windspeed and wind direction, this suggest that the aerosol observed at both sites during the cold period, between 9 and 15 UTC represent the mesoscale to regional aerosol size distribution properties, while during the rest of the day this background aerosol is much more influenced by local emissions that are allowed to accumulate during especially the stagnant periods during the morning and afternoon. The nucleation number appears somewhat higher at Methoni than at Navarino, which is difficult to explain from a process understanding point of view.
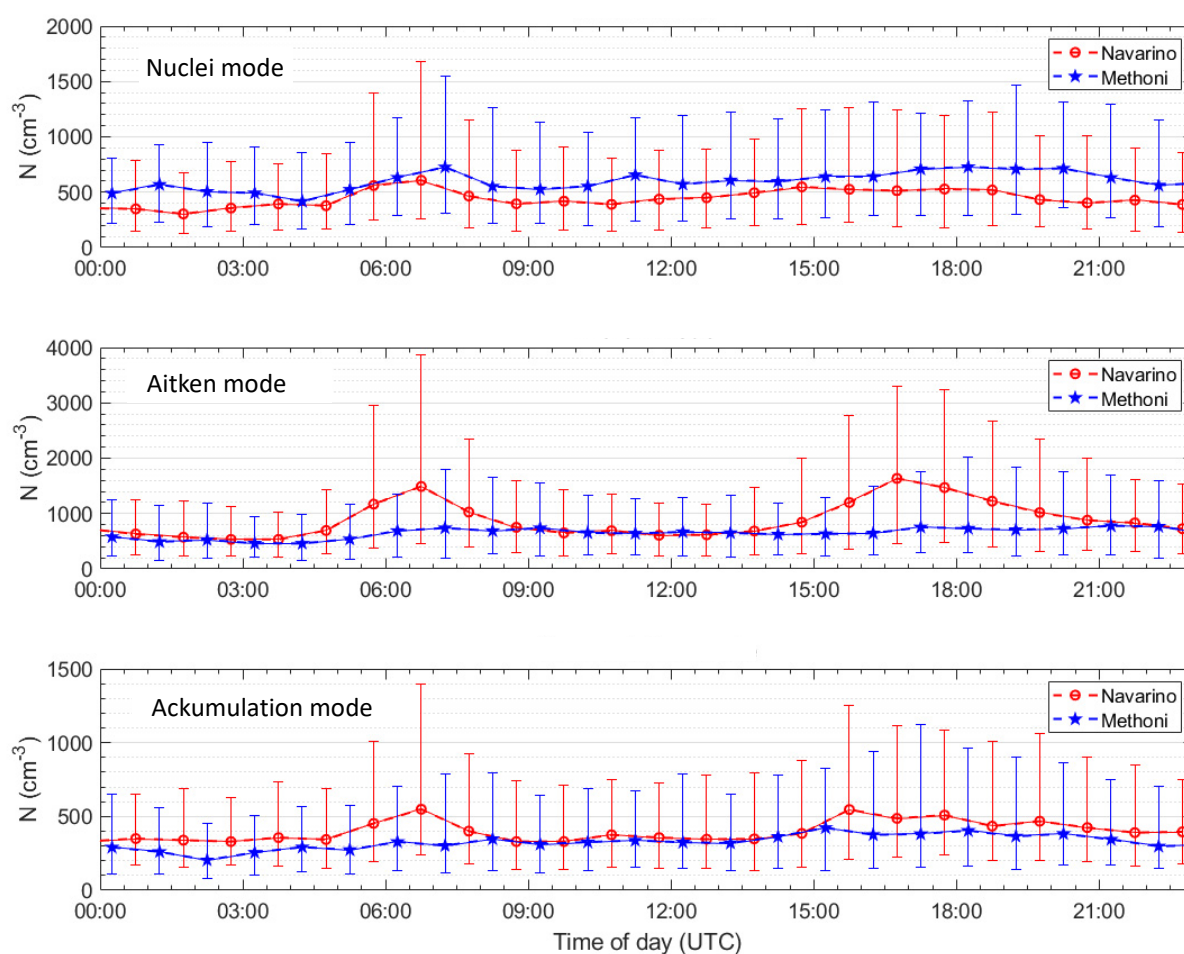

Figure 8. Diurnal variation of number concentration of nuclei, Aitken and accumulation modes for the cold period November–March at Navarino (observations for the period April 2011–September 2013) and at Methoni (observations for the period November 2013–December 2016). The dotted curves indicate the median values while the error bars indicate the inter-quartile range.

During daytime in the cold season with steady sea breeze both the Navarino and the Methoni sites measure the same background air transported mainly over the Adriatic Sea. The concentration of nuclei mode is slightly higher at Methoni during most of the day for unknown reasons while the Aitken and accumulation mode concentrations are the same beside the stagnant periods in the morning and late afternoon at Navarino (Figure 8). However, during the warm period, May to September, Navarino and Methoni show similar concentrations for nuclei mode except during the evening when Navarino is showing higher concentrations (Figure 9). But the Aitken and accumulation number concentrations during the warm period at Navarino are higher than Methoni for the whole

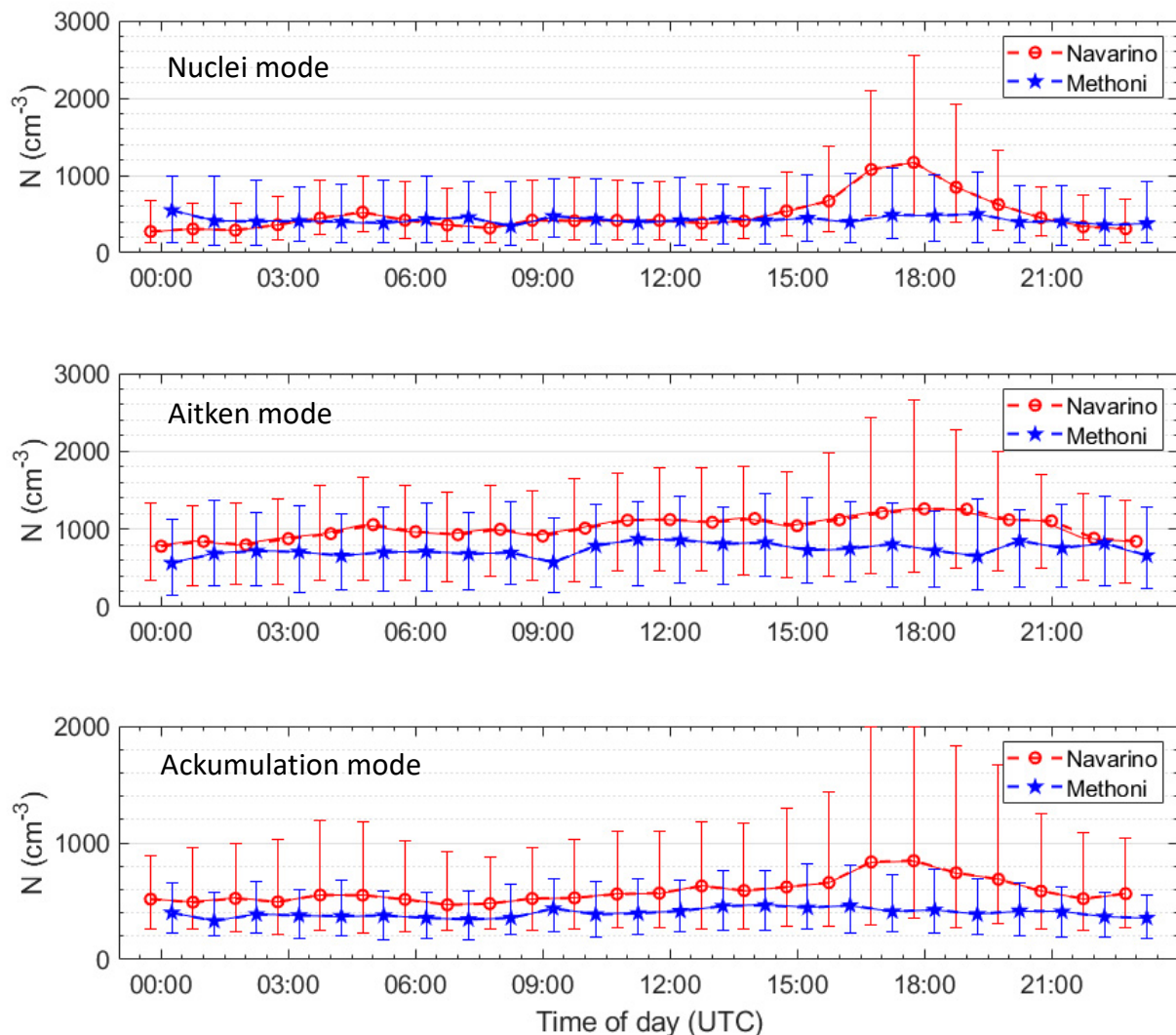day. Even during the steady sea breeze between 9 and 15 UTC Navarino shows about 20% higher concentrations.

Figure 9. Diurnal variation of number concentration of nuclei, Aitken and accumulation modes for the warm period May–September (observations for the period April 2011–September 2013) and at Methoni (observations for the period November 2013–December 2016). The dotted curves indicate the median values while the error bars indicate the inter-quartile range.

The small diurnal variation in the nuclei mode concentrations at Methoni disappears fully during the warm period while it remains at Navarino. The concentrations in all modes seem to slowly increase during the day, which might reflect the effect of the intense photochemistry. A local source or sources along the coast as Navarino is in a large bay where the NW wind sometime follows along the coastline can as well add to the concentrations at Navarino while Methoni seems not to be affected. It appears that this source is considerable larger during the summer than compared with the whole year. It is likely due to more traffic as it is a touristic area.

The monthly mode concentrations between 9 and 15 UTC at Methoni and Navarino agrees for all months but with the general differences shown above (Figure 10). Nuclei mode number is for some unknown reason about 30% higher during the cold period at Methoni, while the Aitken and accumulation mode is 20–30% higher at Navarino during the summer period. Even though the general wind directions in the warm period during daytime is quite similar, Figures 4 and 5 reveal some differences, e.g., at Methoni there is occasionally wind from the ESE. Though, there is a dip in concentrations in August found

at Methoni but also a slight increase at Navarino compared with July and September. This can possibly be due to a low recovery of data in August from Methoni, while at Navarino August is the busiest month at the resort which can cause some local contamination of the measurements.
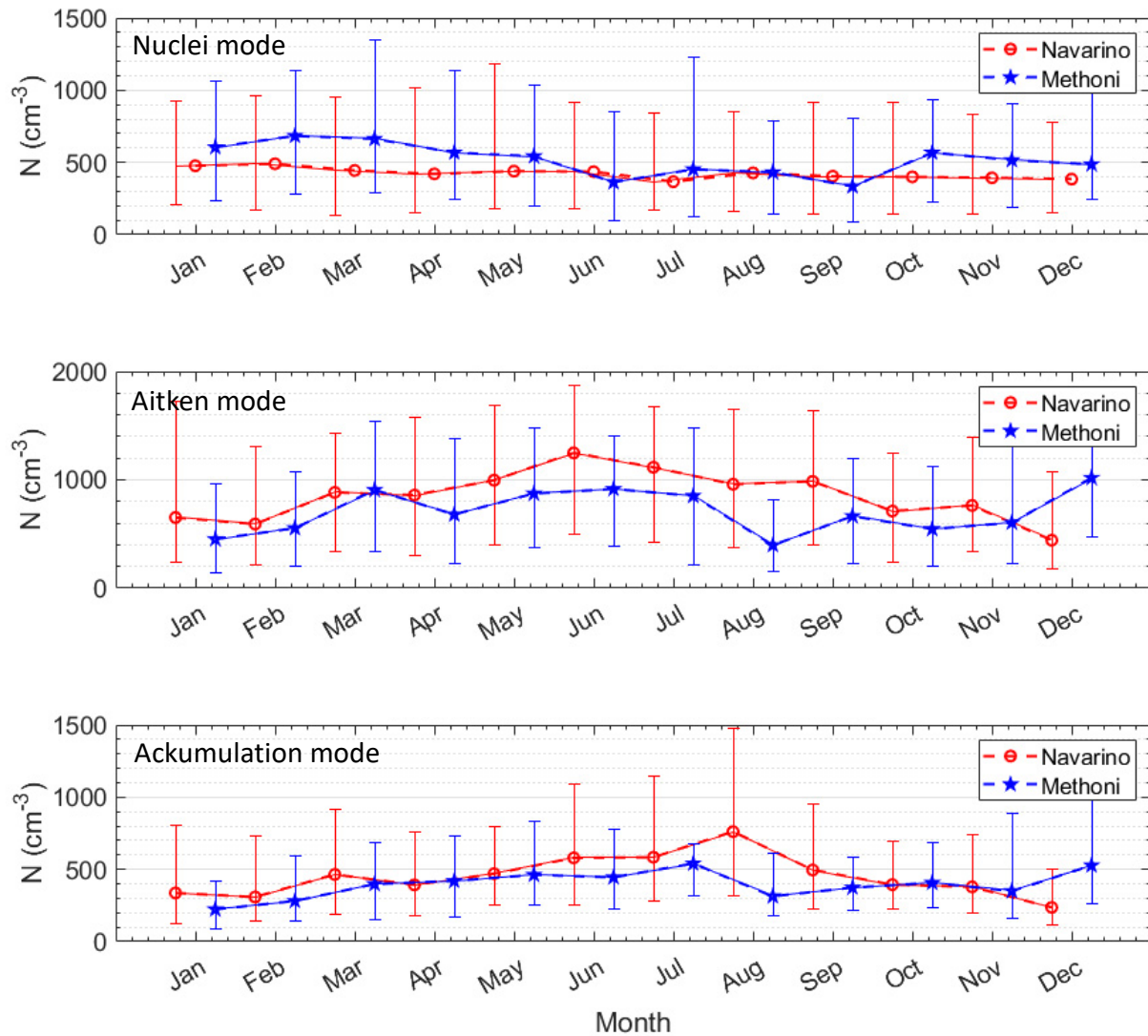

Figure 10. Monthly particle number in the different modes of all measurements between 9 and 15 UTC measured at Navarino and Methoni. The dotted curves indicate the median values while the error bars indicate the inter-quartile range.

At both sites there is a seasonal variation of the total particle number concentration of almost a factor 3 for Aitken and accumulation with the lower concentrations during the winter compared to the summer season. The annual variation, with an increasing total number and mass during spring peaking during the high summer are in line with increasing photochemical production, of condensable and nucleation species.

Considering the main transport route in the winter is over the inland Greece with Athens some 300 km ENE of Navarino and Methoni, while the main route during summer is over the Adriatic Sea originating over central Europe, it is important to note that the concentrations during winter is lower than the summer values (see sections on local meteorology and trajectory analysis).

4.5. Aerosol Number Size Distribution

The monthly mean size distributions for both Methoni and Navarino were calculated using measurements during midday (9–15) (Figure 11). Considering that the measurements cover different periods the two sites agree quite well. Both sites are generally characterized by a bimodal size distribution except for the month of July. This bimodality indicate that the aerosol has gone through one or several cloud-cycles. Some differences are however worth noticing. Firstly, in August Navarino shows more particles and unimodal average number size distribution compared to Methoni. Secondly, a deviation in the size distributions between Navarino and Methoni is also seen during December–January. However, here, Methoni has somewhat higher concentrations in December while Navarino higher in January.
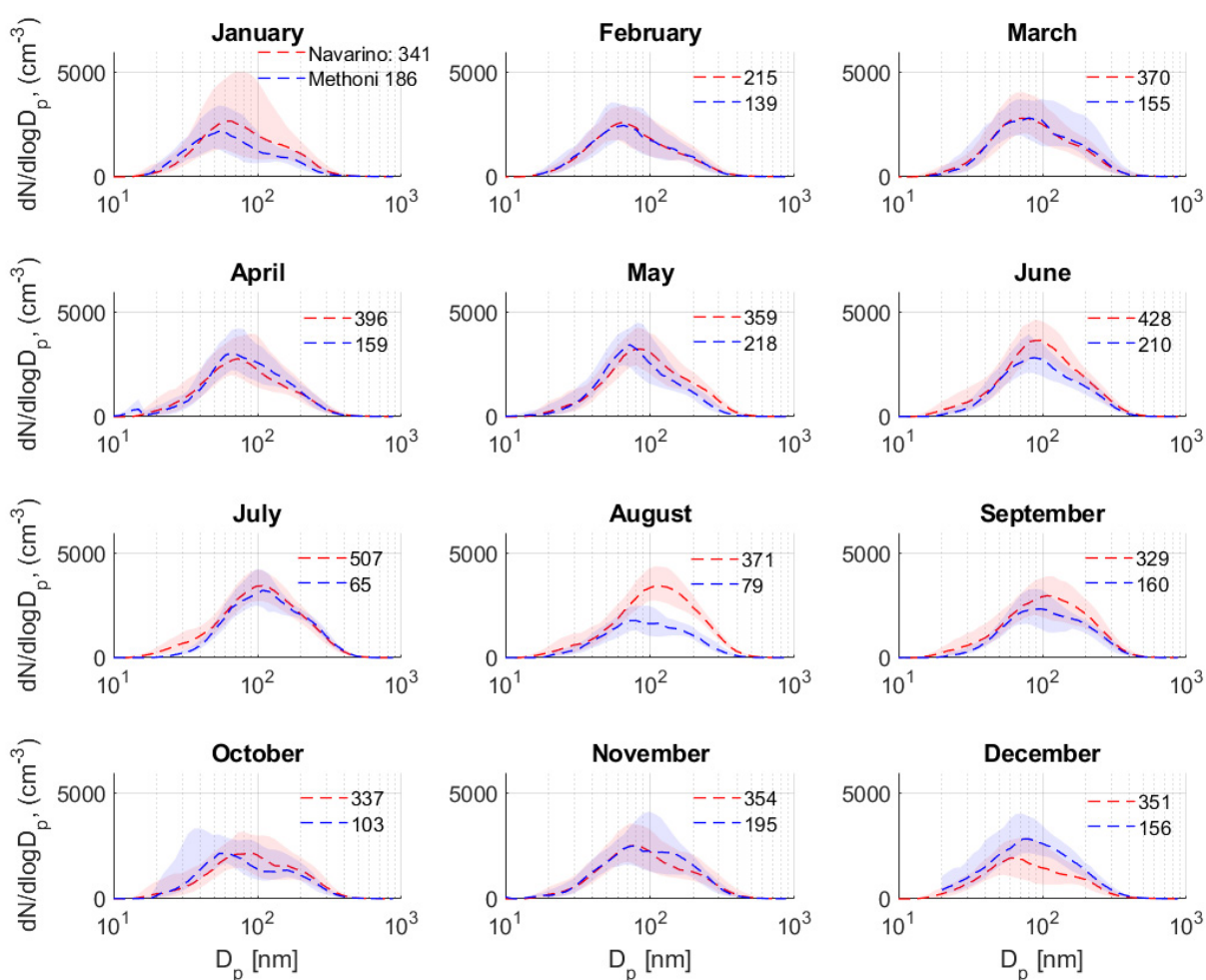

Figure 11. Monthly mean size distributions of measurements between 9 and 15 UTC at Navarino (in red) and Methoni (in blue). The numbers in each frame represents the total amount of hourly average size distributions used in the analysis.

The increased accumulation mode particle and unimodal size distribution during August indicate an influence of local primary accumulation particle at Navarino. At Methoni during the summer the sea breeze is strong and steady often with no change of wind direction during night. Further there is no human activity close to the Methoni site up wind after passing the shore line. However, it should be noted that the data coverage at Methoni during especially August was low. The clearly dominating Aitken mode during June–September with a larger mode diameter than found during the cold period indicate strong photo-chemical production of condensable compounds giving larger Aitken mode particles.

Recalling that Navarino and Methoni represent different observational time series, the differences found in December and January can potentially be explained by the variability in either the long-range transport, the source strength and the local meteorology or a combination of the three.

4.6. Cluster Analysis of Aerosol Size Distributions

Cluster analysis was performed on all size distributions at both sites sampled at midday between 9 and 15 UTC. The choice of six clusters is subjective. Clustering can of course be performed for both fewer and more clusters. However, based on the observed variability of the data, six clusters was considered sufficient to capture the most typical states of the aerosol number size distributions observed at the two sites in the selected sub-set of data. The clustering was performed on normalized size distributions, and the clustering thus converge towards typical shapes of the size distribution. The clusters thus represent the 6 most prevalent occurring size distributions. The quartile range and median of each number size distribution cluster are presented in Figure 12 together with median of all data observed between 09:00 and 15:00 UTC. Note also that the size distribution clusters in Figure 12 are presented as actual $dN/dlogD_p$ values and not the normalized distribution.
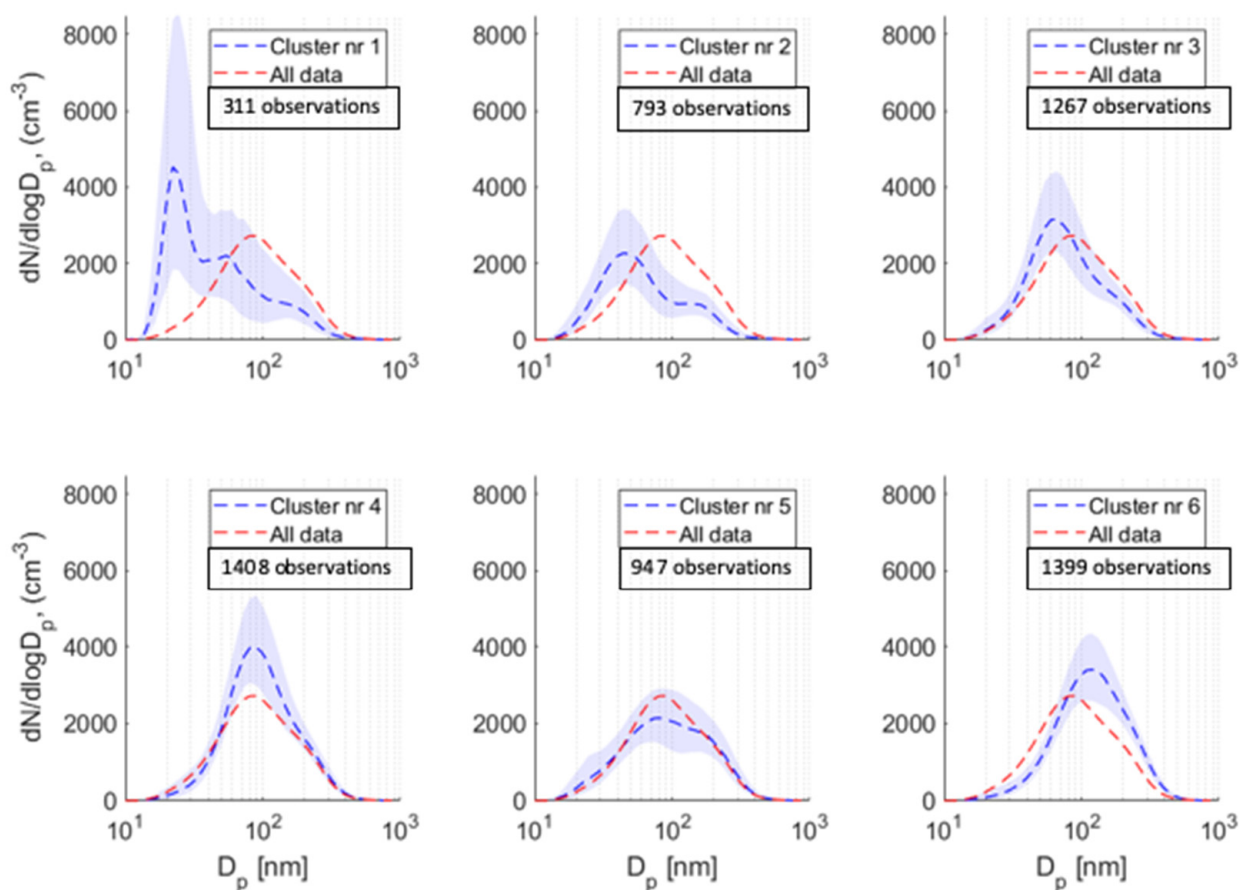

Figure 12. The median of daytime size distribution of cluster 1 to 6 (in blue). The red curve indicate overall median size distribution as reference. The number of members in each cluster is given in the title of each subplot.

Cluster 1 has a clear aged, i.e., larger end of the nucleation mode but also clear indication of cloud processing giving the bimodal structure of an Aitken and accumulation mode with a Hoppel minimum in between. Cluster 2 is similar but without any sign of nucleation. Cluster 3 shows a dominating Aitken mode with a small accumulation mode indication little cloud processing. Cluster 4 shows more aging and more indication of cloud processing, while Cluster 5 shows influence of scavenging, most likely precipitation and

cloud processing. Cluster 6 shows quite aged aerosol with high degree coagulation and condensation and with likely little influence from wet removal processes. All clusters show a significant contribution of particles in the 200 nm range possibly emerging from sea spray as both sites are close to the shore and often exposed to strong on land winds.

The seasonal distribution of cluster members is shown in Figure 13. It is evident that Cluster 1 is most frequently observed during the cold period and exhibits a minimum during summer months. The same seasonal pattern is present for Cluster 2 and Cluster 3. Cluster 4 is rather evenly distributed over the year, although slightly more frequently observed during May–June. Cluster 5 is most common during Autumn/early Winter, while Cluster 6 is typically observed during summer months.
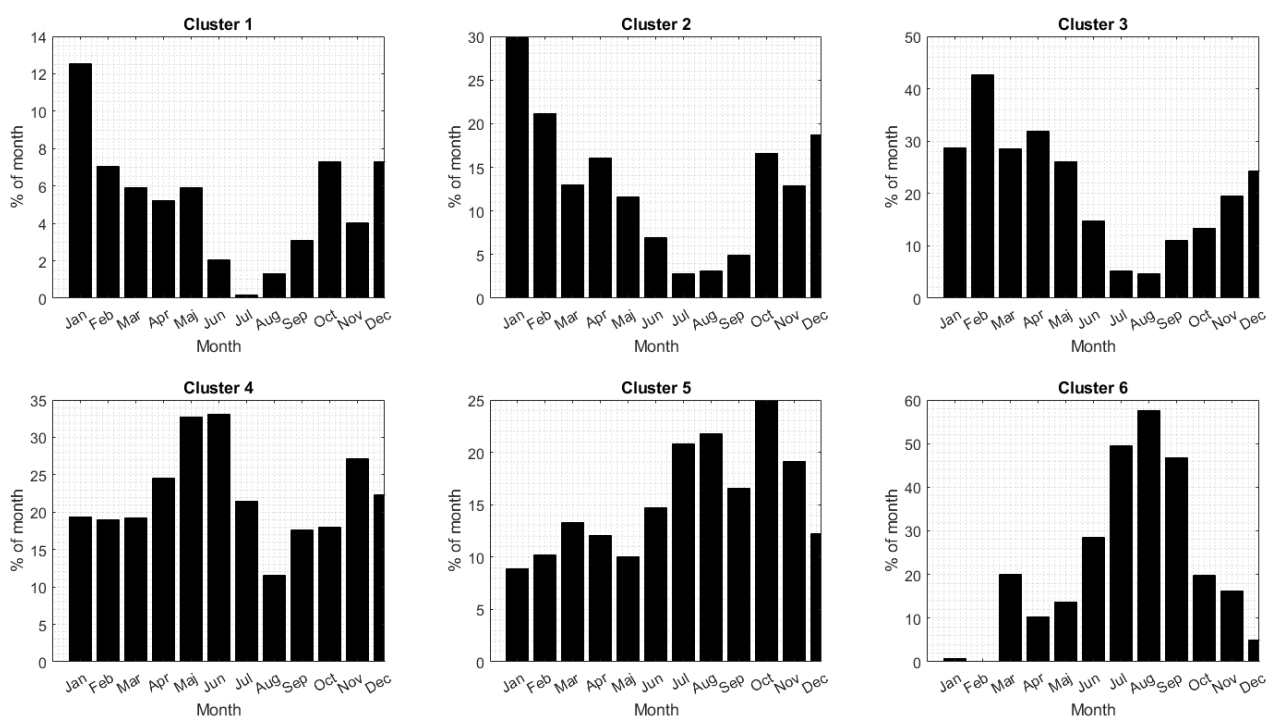

Figure 13. The relative frequency of occurrences of observations belonging to cluster 1–6.

As previously described, each cluster member was associated with an airmass trajectory. This allowed us to calculate statistics on transport related parameters. Figure 14 gives the transport probability function for each cluster. Figure 15 gives the average altitude of trajectory end points belonging to clusters 1 through 6. The average precipitation history along the trajectories belonging to each cluster is given in Figure 16.

Cluster 1 is occurring in airmasses approaching NEO along quite limited transport paths either over southern France from the Atlantic approaching Navarino over the Mediterranean or over the Balkan along the Adriatic coast or the mainland. Some occasions passing from the NE and the Black Sea (Figure 13). The approach is in the boundary layer but it is mainly subsiding air from the free troposphere over the Atlantic that pass over Europe. Another very specific characteristic is that strong precipitation has happened about 20–30 h before arrival to Navarino (Figure 15). Cluster 1 events occur mostly during the cold period, November to March.

The transport pattern and occurrence of cluster 2 is very similar to cluster 1 but with no strong precipitation event before arrival. It is subject to a more even scavenging similar in intensity to cluster 1 during the transport. The lack of strong scavenging, giving higher aerosol concentrations, and thus a larger condensation sink probably prevented nucleation. The cluster 2 event also has a very similar seasonal variation as cluster 1. The main difference compared to cluster 1 seems to be that it has not been exposed to a recent strong precipitation event and it seems to originate from somewhat higher altitude.
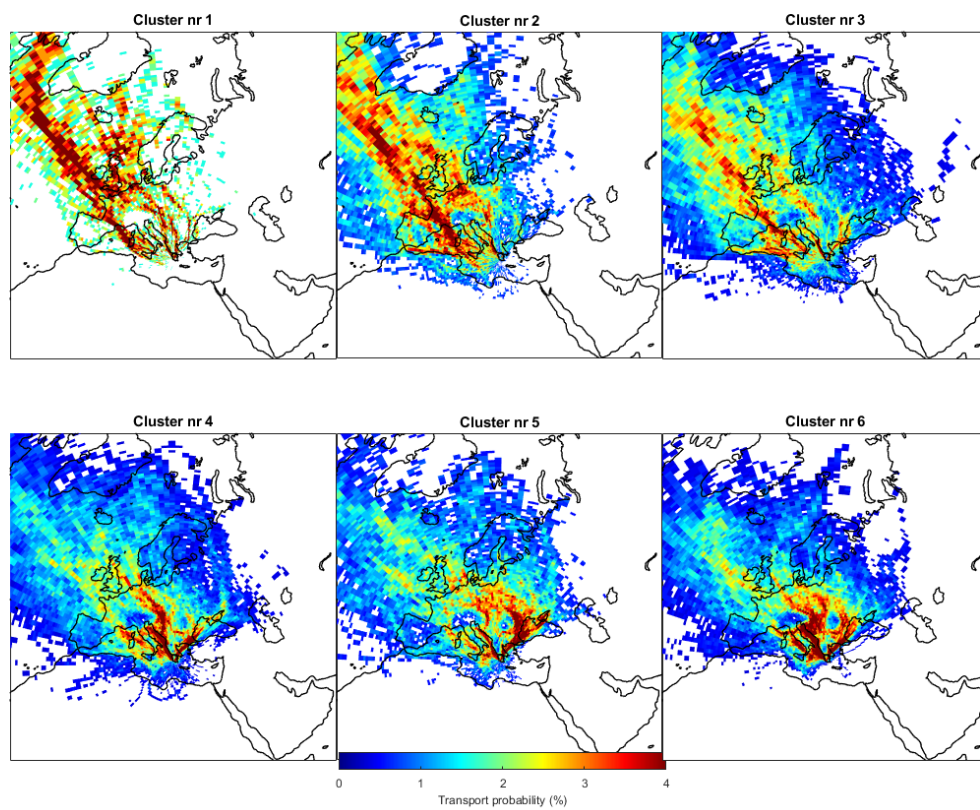
Figure 14. The transport probability, i.e., the probability an air mass trajectory has passed through a grid cell for cluster 1–6.
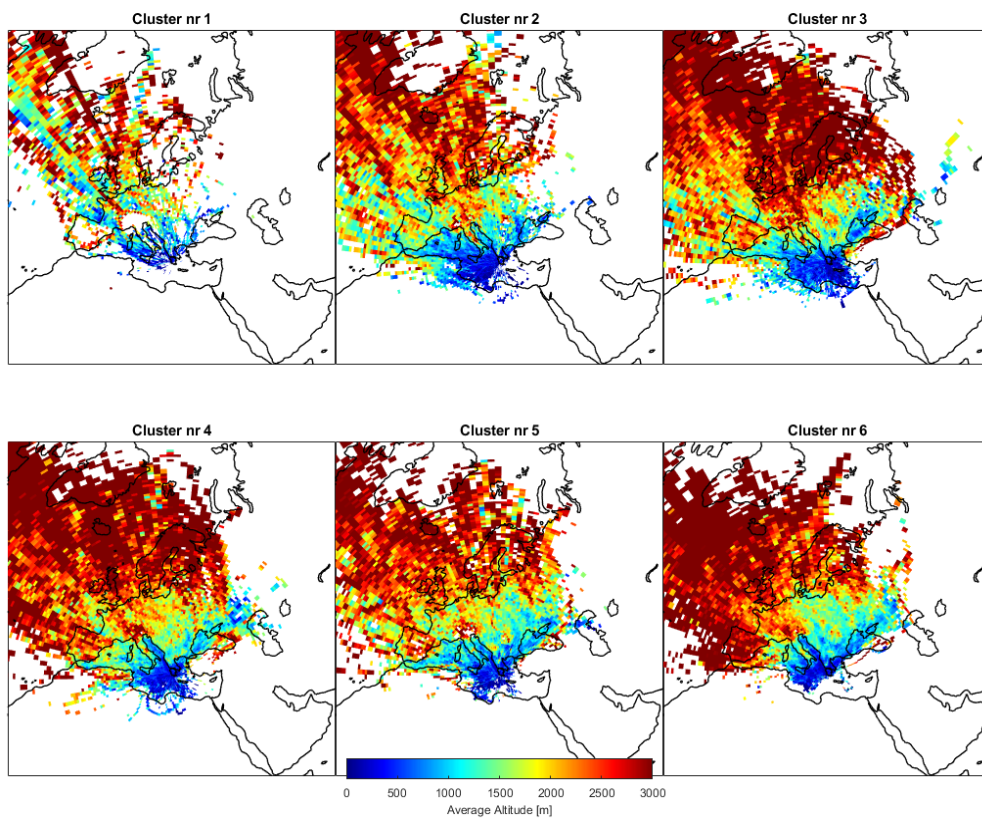

Figure 15. Average altitude for the transport path of the air mass related to cluster 1–6.
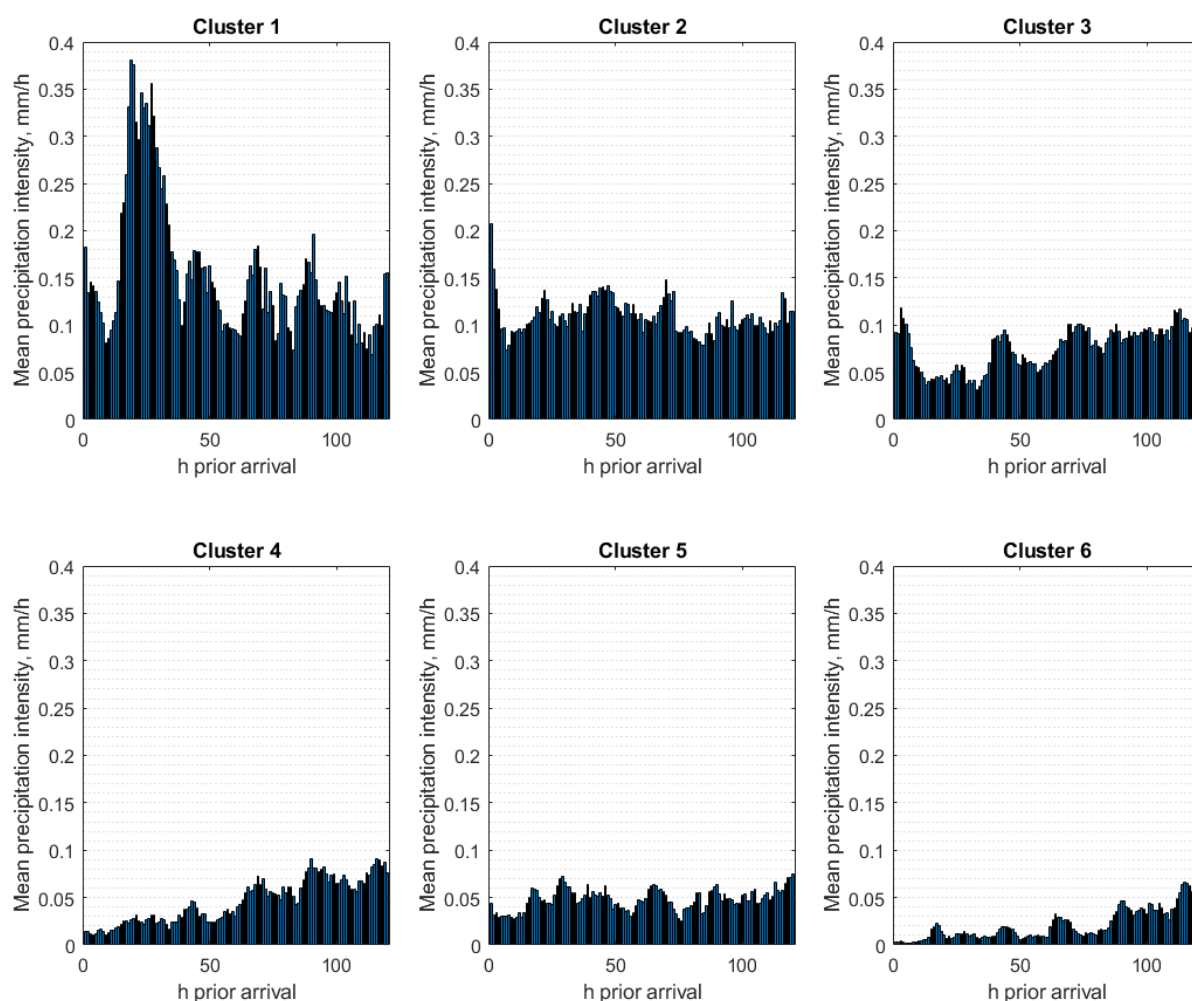
Figure 16. Mean precipitation along the transport of cluster 1 to 6.

Cluster 3 has also a quite similar transport pattern and occurrence as clusters 1 and 2 but been much less exposed to precipitation, about half during the last 40 h during the transport except during the very last hours before arrival. This caused a recent scavenging of the accumulation mode that is dominating the cloud condensation nuclei. Cluster 3 events have a very similar seasonal variation as Cluster 1 and 2 but seem to originate from even higher altitude in the free troposphere.

Clusters 1–3 have strong similarities only varying exposure to precipitation affecting especially the number of accumulation particle number. The air masses have passed over similar areas of European, mostly western or central Europe and most likely picked up emissions over these areas. However, they originate from somewhat different altitude over the Atlantic. These clusters have a clear minimum during the warm period.

Cluster 4 has quite high concentrations of aged Aitken mode particle that originate over the Adriatic or Central Europe subsiding to Navarino but there is also substantial representation of airmasses passing over the Athen/Istanbul area and the very east of Europe. The amount of precipitation is quite low compared with Cluster 1,2 and 3 especially the last two days before the arrival and thus the aerosol has not been especially scavenged. It occurs mostly during the spring–early summer, i.e., in the transition between the cold and warm period and less during the late summer.

The trajectory frequency map of Cluster 5 is quite similar to the map of Cluster 4 but is dominated by air mass transport from the north east over the Balkan passing over Athens and Istanbul. The precipitation is almost as low as for Cluster 4 but occur equally over the whole transport thus is exposed to more scavenging suggesting increased cloud processing.

Cluster 5 occurs less during the midwinter and spring while increasing over the summer into higher occurrence during the fall.

Cluster 4 and 5 are both less exposed to precipitation, arriving in airmasses mostly from the N and NE originating from the central to the eastern Europe. They are occurring during the whole year but Cluster 4 more in the spring while Cluster 5 mostly in the fall.

Cluster 6 is occurring almost only during the warm period originating mainly over Central Europe but also in airmasses from the western and eastern Europe with very little precipitation along the transport giving a very aged unimodal aerosol that has grown to large accumulation particles.

In summary, Clusters 1 through 3 are occurring mostly during the cold period, are transported in a NWN transport sector mostly originating from western or central Europe and have a history of comparably large amounts of precipitation during transport. There are however differences in precipitation history, which affects their size distribution. This is especially true for Cluster 1, where a peak in average precipitation is observed 1–2 days before the arrival to the receptor.

Clusters 4 and 5 occur more evenly throughout the year, while Cluster 6 distributions appear almost exclusively during the warm period. All three are exposed to comparably much lower precipitation. Cluster 6 distributions are influenced by high intensity photochemistry, giving the largest accumulation-mode particles and thus total aerosol mass. Clusters 4 and 5 but also Cluster 6 are substantially influenced by air masses passing over Central/Eastern Europe.

The analysis has focused on the background aerosol and to exclude as much of the local influence as possible it was performed only on aerosol sampled during midday, i.e., 9 to 15 UTC.

4.7. Influence of Precipitation

As shown in the previous section, precipitation history plays a pivotal role for the resulting size distribution observed at the receptor. This is expected as precipitating clouds are the dominating sink for submicron atmospheric aerosols. Thus, frequency and intensity of precipitation influence the atmospheric lifetime of the particles and thus their atmospheric concentrations. It is foremost particle size but also chemistry that control which particles that form cloud droplets and thus will be scavenged in a precipitating cloud. Particles not forming cloud droplets can be scavenged but then due to diffusion, interception or impaction by/on cloud or rain drops. These processes are considerably less efficient compared to acting as cloud condensation nucleus. The updraft velocity in the cloud is very important as it determines the supersaturation reached in the cloud and with that the lower size limit, or rather mass of soluble salts in a particle needed for the particle to be activated. In order to investigate the relation between precipitation history and observed aerosol properties, the last 120 h of precipitation along each cluster trajectory was integrated. These calculated values were in turn paired with aerosol number concentration integrated between 20 and 50 nm, 50–100 nm, 100–400 nm, and >400 nm. The data were subsequently binned according to precipitation experienced during last 5 days, and the relation between experienced precipitation and observed binned number concentration is given in Figure 17.

For the nucleation mode size range (i.e., 10–50 nm), the number of particles show a positive correlation with amount of integrated precipitation up to around 15 mm, when it flattens out. The Aitken mode number concentration show an on average weak decrease with increasing accumulated precipitation. The size ranges denoted 100–400 nm and >400 nm both show strong decrease with increasing precipitation. These results confirm the role of wet removal as the main sink of atmospheric aerosols with a particle size larger than the activation diameter, usually in the 70–100 nm range. The results also suggest that the removal of accumulation mode surface and thus reduction of condensation and coagulation sink through wet deposition favors, at least initially, new particle formation.
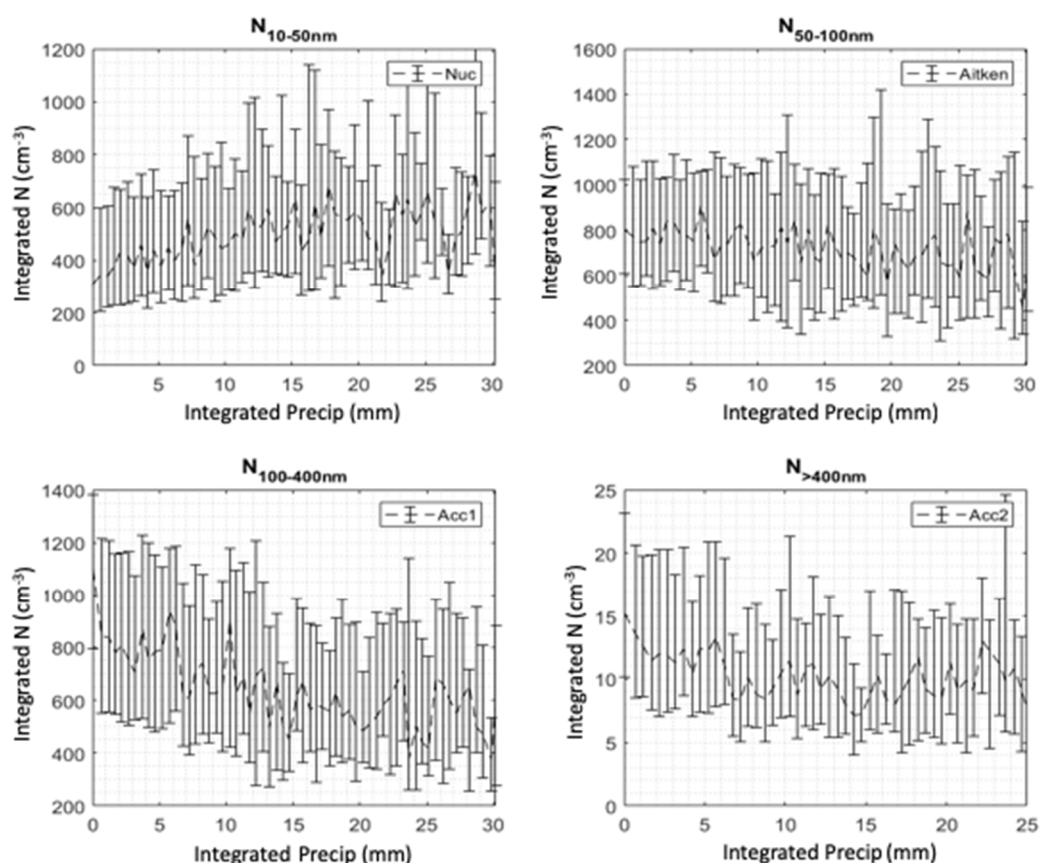
Figure 17. Integrated number concentration over different size and the relation to accumulated precipitation integrated for the last 120 h of transport.

5. Discussion

The eastern Mediterranean is a highly populated area with many environmental challenges including climate change, with not only higher temperature in an already hot area but also changing precipitation patterns, i.e., increasing water deficit in an already arid area.

Air pollution also strongly affects the health of the population. The future development of these environmental threats is of outmost importance for the political and economic development in this region. In developing cost efficient and useful abatement policies reliable projections are essential and the key to this is observations. Observations to detect changes, trends, to develop and evaluate models used for climate and air quality projections. Standardized high-quality measurement of key parameters are needed but it is equally important that the ground-based sites are well characterized and understood. Thus, the local meteorology and influencing factors as local pollution must be well understood and considered when analyzing data for regional background changes.

The meteorology in the Ionian Sea is mostly dominated by northerly subsiding air masses that at the coast are superimposed by the sea land breeze that dominate the local winds during the warm period, May to September but also at times are sustained over large parts of the cold period, November to March. Local topographical features as mountain ranges influence the wind flow and thus how and how much different sites are affected by regional and local sources. These features dominate the local and regional air mass flow at Navarino and Methoni at the west coast of Peloponnese. But even though they are only 20 km apart a considerable difference is found in the influence of the sea breeze pattern due to Methoni being situated on the very tip of the most western peninsula of Peloponnese. As the sea breeze is more persistent, Methoni is more exposed to background air masses transported over the Adriatic. However, it should be remembered when the main air mass

transport is along the Balkan and Italian coasts, the sea land breeze constantly transports emissions from coastal areas into the air masses flowing south over the Adriatic Sea.

The Navarino site being situated within a resort together with the local features of the sea land breeze, make it more sensitive to the local pollution than the Methoni site. Even though the sampling inlet is well above the housing in the resort and no direct emission sources exist in the major wind sector towards the sea, measurements still show increased aerosol concentrations during August, i.e., the major vacation period. Even though the contamination is not dominating during August it cannot be avoided by only using data sampled during the steady strong flow on shore from the NW. However, limiting to midday data, i.e., 9–15 UTC for the rest of the year, the Navarino site gives the same information on background aerosol data as the Methoni site.

During the cold period the main general wind flow is often shifting towards NE, bringing air originating above the eastern Europe as Ukraine and Russia. When passing over the Balkan the air subsides into the boundary layer, and with the sea land breeze it approaches Navarino from the NW. The diurnal sea land breeze wind direction shift causes the wind speed at Navarino to stop while at Methoni the wind speed stays above 2 m/s.

The main anthropogenic emissions affecting the regional air quality observed at NEO originate from different parts of Europe, during the cold period more so from eastern Europe while during the warm period larger contributions come from western and central Europe. NE air masses, which are more frequent during the cold period often pass over Athens and Istanbul thus likely to bring air pollution from these metropolitan areas as well as from the Peloponnese.

The aerosol distributions observed show dependence on their precipitation history. Recent strong precipitation events seem to induce nucleation and subsequent particle growth. Generally, the observations show the amount of precipitation directly decrease the Aitken and accumulation mode particle number while the number of nucleation mode particles increase. The number of particles, total or in the Aitken and accumulation modes are about 2–3 times higher during the warm period. This is most likely reflecting the sun light intensity and with that a more intense photochemistry. This, together with less precipitation, gives a higher aerosol number and mass during the warm period. The nucleation mode particle number shows indications to decrease during the summer, which is probably due to higher aerosol concentrations and with that a larger condensation sink.

6. Conclusions

The observed background aerosol is originating from aged European aerosols and is strongly influenced by anthropogenic activities such as biomass burning, fossil fuel combustion, and industry. When entering the boundary layer over the Adriatic Sea, local sources contribute to air pollution in the air masses moving south. Seasonal variation in source strength (e.g., local/regional agricultural burning of biomass) typically affects the aerosol. Meteorological phenomena seem furthermore to have a strong impact on the aerosol:

- Mesoscale meteorology determines the diurnal variation of aerosol properties such as mass and number by means of typical sea land breeze circulation, giving rise to pronounced morning and evening peaks in pollutant levels.
- Synoptic scale meteorology, mainly large-scale air mass transport and precipitation, strongly influence the seasonality of the aerosol properties.
- Precipitation likely stimulates new particle formation by the reduction of condensation sink.

A more general conclusion to draw from this investigation is that even though the air over the Ionic and Adriatic Seas seems clean and fresh it is still strongly contaminated by Central European and regional air pollution affecting air quality and climate in a large part of the Mediterranean.

Appendix A. Aerosol Size Distributions

The aerosol size distributions for the cold and warm periods show quite similar feature. However, the warm period shows somewhat higher concentrations, with Navarino at about 3000 cm^{-3} and peaking at 100 nm while Methoni have a mean concentration of about 2500 cm^{-3} and a mean size of 80 nm. During the cold season, the mean particle size is about 80 nm for both while Navarino has slightly higher concentrations of 2700 cm^{-3} compared to 2500 cm^{-3} for Methoni (Figure A1).
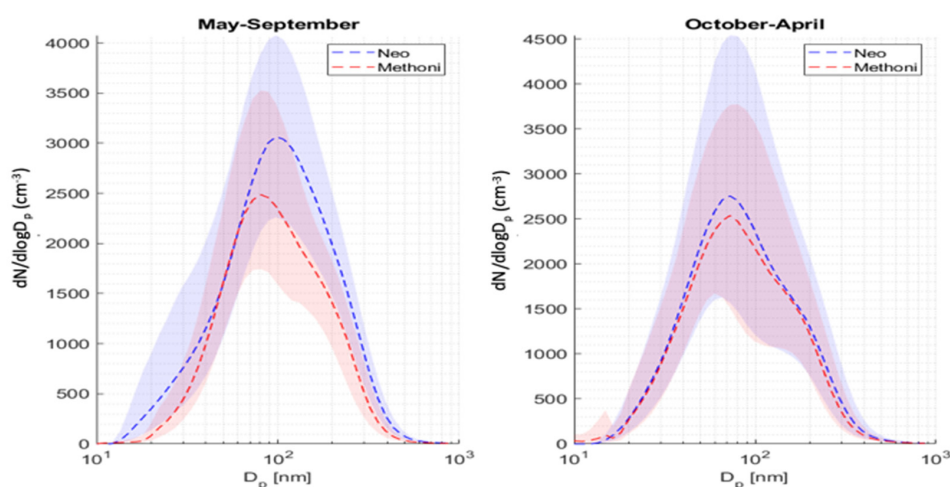

Figure A1. Seasonal averages for aerosol number size distributions observed at NAVARINO and Methoni, respectively. Colored areas indicate 25–75th percentile ranges and dashed line represent median.

Through fitting 3 modes, interpret as nuclei, Aitken and accumulation mode, following data was calculated as given below.

Table A1. Fitted modal parameters for NAVARINO, 2011–16 November 2013. (GSD stands for Geometric Standard Deviation and Dg for particle diameter as measured by a Differential Mobility Analyzer).

	N (cm⁻³)		GSD		Dg (nm)		N (cm⁻³)		GSD		Dg (nm)	
January												
Nuclei	500	(219–1099)	1.3	(1.21–1.449)	39	(28–54)	430	(186–974)	1.4	(1.24–1.645)	34	(26–61)
Aitken	780	(286–1992)	1.5	(1.3–1.756)	75	(61–90)	1042	(378–1668)	1.48	(1.28–1.735)	96	(76–113)
Accumulation	394	(158–930)	1.43	(1.31–1.637)	161	(122–198)	573	(253–1233)	1.43	(1.32–1.601)	186	(139–238)
February												
Nuclei	461	(180–971)	1.35	(1.23–1.541)	47	(32–60)	467	(202–1051)	1.39	(1.23–1.635)	34	(26–57)
Aitken	704	(266–1488)	1.49	(1.29–1.78)	77	(64–97)	1011	(372–1733)	1.48	(1.27–1.734)	94	(73–116)
Accumulation	339	(147–772)	1.45	(1.31–1.643)	168	(127–206)	785	(357–1505)	1.46	(1.34–1.604)	181	(143–226)
March												
Nuclei	431	(159–986)	1.34	(1.22–1.534)	46	(29–65)	444	(179–950)	1.36	(1.22–1.588)	36	(26–61)
Aitken	980	(350–1797)	1.5	(1.31–1.774)	80	(67–98)	911	(376–1521)	1.48	(1.29–1.742)	91	(71–112)
Accumulation	479	(201–1027)	1.43	(1.32–1.609)	175	(127–210)	553	(259–1084)	1.42	(1.33–1.563)	191	(150–226)
April												
Nuclei	469	(176–1038)	1.33	(1.21–1.52)	41	(28–59)	434	(166–907)	1.34	(1.22–1.539)	42	(28–64)
Aitken	947	(324–1715)	1.48	(1.3–1.759)	79	(65–98)	757	(277–1411)	1.49	(1.29–1.735)	81	(67–104)
Accumulation	415	(171–870)	1.44	(1.32–1.626)	168	(125–212)	392	(209–699)	1.39	(1.31–1.509)	195	(155–226)
May												
Nuclei	452	(192–1026)	1.33	(1.22–1.528)	39	(27–60)	405	(147–956)	1.34	(1.21–1.541)	50	(30–66)
Aitken	989	(385–1611)	1.45	(1.29–1.697)	86	(71–104)	904	(350–1970)	1.53	(1.33–1.753)	81	(70–97)
Accumulation	466	(249–813)	1.42	(1.33–1.57)	192	(153–232)	421	(212–841)	1.42	(1.32–1.544)	197	(157–227)
June												
Nuclei	472	(196–983)	1.36	(1.23–1.589)	35	(25–59)	398	(166–878)	1.35	(1.23–1.526)	42	(29–58)
Aitken	1026	(378–1696)	1.45	(1.28–1.715)	88	(71–109)	615	(211–1545)	1.51	(1.3–1.768)	78	(64–96)
Accumulation	546	(225–1138)	1.44	(1.32–1.615)	180	(134–230)	305	(137–616)	1.4	(1.3–1.566)	173	(135–210)

Table A2. Fitted modal parameters for Methoni, December 2013–2016.

	N (cm⁻³)		GSD		Dg (nm)		N (cm⁻³)		GSD		Dg (nm)	
January						**July**						
Nuclei	609	(266–1061)	1.46	(1.28–1.645)	44	(30–56)	412	(103–1148)	1.4	(1.22–1.589)	68	(42–88)
Aitken	453	(167–1029)	1.42	(1.25–1.78)	74	(56–105)	809	(227–1431)	1.47	(1.27–1.651)	108	(92–128)
Accumulation	216	(85–417)	1.38	(1.27–1.556)	164	(133–200)	445	(273–722)	1.37	(1.29–1.445)	227	(197–250)
February						**August**						
Nuclei	598	(259–1073)	1.4	(1.25–1.566)	46	(30–59)	421	(121–809)	1.42	(1.24–1.589)	59	(39–76)
Aitken	550	(208–1121)	1.43	(1.25–1.757)	76	(62–97)	449	(153–894)	1.46	(1.25–1.699)	93	(74–119)
Accumulation	257	(104–551)	1.4	(1.27–1.562)	168	(135–209)	341	(183–544)	1.35	(1.28–1.441)	191	(167–223)
March						**September**						
Nuclei	714	(251–1310)	1.36	(1.23–1.558)	50	(33–68)	369	(105–821)	1.4	(1.23–1.595)	57	(38–75)
Aitken	836	(300–1629)	1.5	(1.28–1.752)	88	(64–118)	588	(162–1148)	1.47	(1.26–1.682)	97	(78–115)
Accumulation	412	(177–782)	1.39	(1.3–1.51)	183	(153–218)	326	(193–521)	1.36	(1.28–1.454)	199	(171–233)
April						**October**						
Nuclei	576	(220–1279)	1.37	(1.24–1.557)	53	(29–65)	485	(228–884)	1.34	(1.19–1.554)	45	(28–58)
Aitken	706	(258–1465)	1.45	(1.26–1.732)	80	(66–104)	600	(212–1117)	1.44	(1.28–1.693)	75	(54–100)
Accumulation	412	(144–719)	1.41	(1.31–1.548)	171	(134–212)	346	(182–594)	1.41	(1.31–1.55)	169	(141–202)
May						**November**						
Nuclei	559	(195–1153)	1.33	(1.22–1.533)	46	(30–63)	506	(198–889)	1.42	(1.23–1.664)	47	(33–67)
Aitken	819	(340–1492)	1.41	(1.27–1.631)	79	(65–95)	644	(223–1446)	1.52	(1.26–1.848)	85	(67–107)
Accumulation	426	(202–767)	1.41	(1.31–1.563)	162	(124–203)	350	(152–905)	1.4	(1.27–1.555)	174	(139–208)
June						**December**						
Nuclei	340	(105–832)	1.32	(1.2–1.503)	50	(33–69)	583	(250–1443)	1.39	(1.25–1.775)	39	(26–66)
Aitken	849	(327–1409)	1.47	(1.29–1.667)	87	(73–105)	921	(316–1714)	1.47	(1.27–1.782)	79	(64–95)
Accumulation	446	(224–719)	1.39	(1.3–1.556)	189	(146–220)	496	(212–1074)	1.43	(1.3–1.594)	166	(124–206)

References

1. Kanakidou, M.; Mihalopoulos, N.; Kindap, T.; Im, U.; Vrekoussis, M.; Gerasopoulos, E.; Dermitzaki, E.; Unal, A.; Koçak, M.; Markakis, K.; et al. Megacities as hot spots of air pollution in the East Mediterranean. *Atmos. Environ.* **2011**, *45*, 1223–1235. [CrossRef]
2. Asmi, A.; Wiedensohler, A.; Laj, P.; Fjaeraa, A.-M.; Sellegri, K.; Birmili, W.; Weingartner, E.; Baltensperger, U.; Zdimal, V.; Zikova, N.; et al. Number size distributions and seasonality of submicron particles in Europe 2008–2009. *Atmos. Chem. Phys. Discuss.* **2011**, *11*, 5505–5538. [CrossRef]
3. Solomon, S.; Plattner, G.K.; Knutti, R.; Friedlingstein, P. Irreversible climate change due to carbon dioxide emissions. *Proc. Natl. Acad. Sci. USA* **2009**, *106*, 1704–1709. [CrossRef]
4. Nastos, P.; Zerefos, C. Spatial and temporal variability of consecutive dry and wet days in Greece. *Atmos. Res.* **2009**, *94*, 616–628. [CrossRef]
5. Kostopoulou, E.; Jones, P.D. Comprehensive analysis of the climate variability in the eastern Mediterranean. Part I: Map-pattern classification. *Int. J. Clim.* **2007**, *27*, 1189–1214. [CrossRef]
6. Navarro, J.C.A.; Varma, V.; Riipinen, I.; Seland, Ø.; Kirkevåg, A.; Struthers, H.; Iversen, T.; Hansson, H.-C.; Ekman, A.M.L. Amplification of Arctic warming by past air pollution reductions in Europe. *Nat. Geosci.* **2016**, *9*, 277–281. [CrossRef]
7. Helmis, C.G.; Moussiopoulos, N.; Flocas, H.A.; Sahm, P.; Assimakopoulos, V.D.; Naneris, C.; Maheras, P. Estimation of transboundary air pollution on the basis of synoptic-scale weather types. *Int. J. Clim.* **2003**, *23*, 405–416. [CrossRef]
8. Lelieveld, J.; Berresheim, H.; Borrmann, S.; Crutzen, P.J.; Dentener, F.J.; Fischer, H.; Feichter, J.; Flatau, P.J.; Heland, J.; Holzinger, R.; et al. Global Air Pollution Crossroads over the Mediterranean. *Science* **2002**, *298*, 794–799. [CrossRef]
9. Hildebrandt, L.; Kostenidou, E.; Mihalopoulos, N.; Worsnop, D.R.; Donahue, N.M.P.; Pandis, S.N. Formation of highly oxygenated organic aerosol in the atmosphere: Insights from the Finokalia Aerosol Measurement Experiments. *Geophys. Res. Lett.* **2010**, *37*. [CrossRef]
10. Carbo, P.; Krom, M.D.; Homoky, W.B.; Benning, L.G.; Herut, B. Impact of atmospheric deposition on N and P geochemistry in the southeastern Levantine basin. *Deep. Sea Res. Part II: Top. Stud. Oceanogr.* **2005**, *52*, 3041–3053. [CrossRef]
11. Theodosi, C.; Im, U.; Bougiatioti, A.; Zarmpas, P.; Yenigun, O.; Mihalopoulos, N. Aerosol chemical composition over Istanbul. *Sci. Total. Environ.* **2010**, *408*, 2482–2491. [CrossRef]
12. Theodosi, C.; Grivas, G.; Zarmpas, P.; Chaloulakou, A.; Mihalopoulos, N. Mass and chemical composition of size-segregated aerosols (PM1, PM2.5, PM10) over Athens, Greece: Local versus regional sources. *Atmos. Chem. Phys.* **2011**, *11*, 11895–11911. [CrossRef]
13. Koçak, M.; Mihalopoulos, N.; Kubilay, N. Origin and source regions of PM10 in the Eastern Mediterranean atmosphere. *Atmos. Res.* **2009**, *92*, 464–474. [CrossRef]
14. Mihalopoulos, N.; Stephanou, E.; Kanakidou, M.; Pilitsidis, S.; Bousquet, P. Tropospheric aerosol ionic composition above the Eastern Mediterranean Area. *Tellus* **1997**, *49B*, 314–326. [CrossRef]
15. Koulouri, E.; Saarikoski, S.; Theodosi, C.; Markaki, Z.; Gerasopoulos, E.; Kouvarakis, G.; Mäkelä, T.; Hillamo, R.; Mihalopoulos, N. Chemical composition and sources of fine and coarse aerosol particles in the Eastern Mediterranean. *Atmospheric Environ.* **2008**, *42*, 6542–6550. [CrossRef]
16. Eleftheriadis, K.; Colbeck, I.; Housiadas, C.; Lazaridis, M.; Mihalopoulos, N.; Mitsakou, C.; Smolík, J.; Ždímal, V. Size distribution, composition and origin of the submicronaerosol in the marine boundary layer during the eastern Mediterranean "SUB-AERO" experiment. *Atmos. Environ.* **2006**, *40*, 6245–6260. [CrossRef]
17. Lazaridis, M.; Eleftheriadis, K.; Smolik, J.; Colbeck, I.; Kallos, G.; Drossinos, I.; Zdimal, V.; Vecera, Z.; Mihalopoulos, N.; Mikuska, P.; et al. Dynamics of fine particles and photo-oxidants in the Eastern Mediterranean (SUB-AERO). *Atmos. Environ.* **2006**, *40*, 6214–6228. [CrossRef]
18. Kalivitis, N.; Kerminen, V.-M.; Kouvarakis, G.; Stavroulas, I.; Tzitzikalaki, E.; Kalkavouras, P.; Daskalakis, N.; Myriokefalitakis, S.; Bougiatioti, A.; Manninen, H.E.; et al. Formation and growth of atmospheric nanoparticles in the eastern Mediterranean: Results from long-term measurements and process simulations. *Atmos. Chem. Phys.* **2019**, *19*, 2671–2686. [CrossRef]
19. Kopanakis, I.; Eleftheriadis, K.; Mihalopoulos, N.; Lydakis-Simantiris, N.; Katsivela, E.; Pentari, D.; Zarmpas, P.; Lazaridis, M. Physico-chemical characteristics of particulate matter in the Eastern Mediterranean. *Atmospheric Res.* **2012**, *106*, 93–107. [CrossRef]
20. Pikridas, M.; Riipinen, I.; Hildebrandt, L.; Kostenidou, E.; Manninen, H.; Mihalopoulos, N.; Kalivitis, N.; Burkhart, J.F.; Stohl, A.; Kulmala, M.; et al. New particle formation at a remote site in the eastern Mediterranean. *J. Geophys. Res. Space Phys.* **2012**, *117*. [CrossRef]
21. Petäjä, T.; Kerminen, V.-M.; Dal Maso, M.; Junninen, H.; Koponen, I.K.; Hussein, T.; Aalto, P.P.; Andronopoulos, S.; Robin, D.; Hämeri, K.; et al. Sub-micron atmospheric aerosols in the surroundings of Marseille and Ath-ens: Physical characterization and new particle formation. *Atmos. Chem. Phys.* **2007**, *7*, 2705–2720. [CrossRef]
22. Siakavaras, D.; Samara, C.; Petrakakis, M.; Biskos, G. Nucleation events at a coastal city during the warm period: Kerbside versus urban background measurements. *Atmos. Environ.* **2016**, *140*, 60–68. [CrossRef]
23. Kalivitis, N.; Kerminen, V.-M.; Kouvarakis, G.; Stavroulas, I.; Bougiatioti, A.; Nenes, A.; Manninen, H.E.; Petäjä, T.; Kulmala, M.; Mihalopoulos, N. Atmospheric new particle formation as a source of CCN in the eastern Mediterranean marine boundary layer. *Atmos. Chem. Phys.* **2015**, *15*, 9203–9215. [CrossRef]

24. Kalkavouras, P.; Bossioli, E.; Bezantakos, S.; Bougiatioti, A.; Kalivitis, N.; Stavroulas, I.; Kouvarakis, G.; Protonotariou, A.P.; Dandou, A.; Biskos, G.; et al. New particle formation in the southern Aegean Sea during the Etesians: Importance for CCN production and cloud droplet number. *Atmos. Chem. Phys.* **2017**, *17*, 175–192. [CrossRef]
25. Tunved, P.; Ström, J.; Krejci, R. Arctic aerosol life cycle: Linking aerosol size distributions observed between 2000 and 2010 with air mass transport and precipitation at Zeppelin station, Ny-Ålesund, Svalbard. *Atmos. Chem. Phys. Discuss.* **2013**, *13*, 3643–3660. [CrossRef]
26. Jokinen, V.; Mäkelä, J.M. Closed-loop arrangement with critical orifice for DMA sheath/excess flow system. *J. Aerosol Sci.* **1997**, *28*, 643–648. [CrossRef]
27. Draxier, R.R.; Hess, G.D. An overview of the HYSPLIT_4 modelling system for trajectories, dispersion and deposition. *Aust. Meteorol. Mag.* **1998**, *47*, 295–308.
28. Tunved, P.; Ström, J.; Hansson, H.-C. An investigation of processes controlling the evolution of the boundary layer aer-osol size distribution properties at the Swedish background station Aspvreten. *Atmos. Chem. Phys.* **2004**, *4*, 2581–2592. [CrossRef]
29. Beddows, D.C.S.; Dall'Osto, M.; Harrison, R.M. Cluster Analysis of Rural, Urban and Curbside Atmospheric Particle Size Data. *Environ. Sci. Technol.* **2009**, *43*, 4694–4700. [CrossRef]
30. Freud, E.; Krejci, R.; Tunved, P.; Leaitch, W.R.; Nguyen, Q.T.; Massling, A.; Skov, H.; Barrie, L. Pan-Arctic aerosol number size distributions: Seasonality and transport patterns. *Atmos. Chem. Phys. Discuss.* **2017**, *17*, 8101–8128. [CrossRef]
31. Rizzo, L.V.; Roldin, P.; Brito, J.; Backman, J.; Swietlicki, E.; Krejci, R.; Tunved, P.; Petäjä, T.; Kulmala, M.; Artaxo, P. Multi-year statistical and modeling analysis of submicrometer aerosol number size distributions at a rain forest site in Amazonia. *Atmos. Chem. Phys. Discuss.* **2018**, *18*, 10255–10274. [CrossRef]